

1 **MUDA: dynamic geophysical and geochemical MUltiparametric DAtabase**

Marco Massa⁽¹⁾, Andrea Luca Rizzo^(1,2), Davide Scafidi⁽³⁾, Elisa Ferrari⁽¹⁾, Sara Lovati⁽¹⁾, Lucia Luzi⁽¹⁾ and MUDA WG (*)

2

3 ⁽¹⁾ National Institute of Geophysics and Volcanology (INGV), Milano department, Italy

⁽²⁾ University of Milano Bicocca, DISAT, Milano, Italy

⁽³⁾ University of Genova, DISTAV, Genova, Italy

4

5 (*) A full list of authors appears at the end of the paper

6

7 Corresponding author: marco.massa@ingv.it

8

9 **Abstract**

10 In this paper, the new dynamic geophysical and geochemical MUltiparametric DAtabase
11 (MUDA) is presented. MUDA is a new infrastructure of the National Institute of Geophysics and
12 Volcanology (INGV), published on-line in December 2023, with the aim of archiving and
13 disseminating multiparametric data collected by multidisciplinary monitoring networks. MUDA is a
14 *MySQL* relational database with a web interface developed in *php*, aimed at investigating in quasi real
15 time possible correlations between seismic phenomena and variations in endogenous and
16 environmental parameters. At present, MUDA collects data from different types of sensors such as
17 hydrogeochemical probes for physical-chemical parameters in waters, meteorological stations,
18 detectors of air Radon concentration, diffusive flux of carbon dioxide (CO₂) and seismometers
19 belonging both to the National Seismic Network of INGV and to temporary networks installed in the
20 framework of multidisciplinary research projects. MUDA daily publishes data updated to the previous
21 day and offers the chance to view and download multiparametric time series selected for different
22 time periods. The resultant dataset provides broad perspectives in the framework of future high
23 frequency and continuous multiparametric monitoring as a starting point to identify possible seismic

24 precursors for short-term earthquake forecasting. MUDA is now quoted with the Digital Object
25 Identifier <https://doi.org/10.13127/muda> (Massa et al., 2023).

26

27 **Key words:** multiparametric data, monitoring networks, dynamic data base, earthquakes forecasting

28

29 **1 Introduction**

30

31 Today, there is an increasing awareness of the role played by the interaction between tectonics
32 and fluid dynamics in triggering seismicity. Yet, the simultaneous monitoring of the relevant key
33 factors is still lacking, even though it could be crucial in recognizing precursory signals. Changes in
34 water chemistry and levels, spring discharges, soil flux regimes (e.g. CO₂, CH₄, Radon) and
35 compositions of dissolved gases in water are well-documented in the literature (e.g. Italiano et al.,
36 2001, 2004; Chiodini et al., 2020; Gori and Barberio, 2022 and references therein), as being pre-, co-
37 and post-seismic modifications as well as markers of the local tectonic stress acting in the crust. These
38 recognized seismic-induced variations in groundwaters and springs led, in recent years, scientists to
39 give more attention to the development of multiparametric monitoring, in order to capture the main
40 evidences concerning abrupt changes in chemical and physical parameters recorded before (and also
41 after) energetic seismic events (Rikitake and Hamada, 2003; Cicerone et al., 2009; Martinelli, 2018
42 and references therein). The ultimate goal is to find systematic signals that can be assumed as possible
43 “precursors” or indicators that a seismogenetic process is ongoing (Hubbert and Rubey, 1959; Brauer
44 et al., 2003; Miller et al., 2004; Chiarabba et al., 2009; Di Luccio et al., 2010; Malagnini et al., 2012;
45 Keranen and Weingarten, 2018; Napolitano et al., 2020; De Matteis et al., 2021; Gabrielli et al., 2022,
46 2023; Ventura and Di Giovambattista, 2013). At the Italian scale, several studies have described the
47 utility of groundwater and spring parameters and soil gas emissions to catch seismic-related signals
48 as well. However, only a few studies reported a continuous, high-frequency monitoring, mainly of
49 groundwater level or hydraulic pressure (De Gregorio et al., 2012; Barberio et al., 2017; De Luca et

50 al., 2018), or as Gori and Barberio (2022) concerning spring monitoring (i.e. temperature, pH,
51 electrical conductivity, dissolved oxygen and carbon dioxide) or D'Alessandro et al. (2020) on soil
52 Radon emissions related to seismic activity.

53 MUDA (geophysical and geochemical MULTiparametric DAtabase), a new dynamic
54 multiparametric database published on-line in December 2023 at the web site <https://muda.mi.ingv.it>
55 (Figure 1), has been developed in such a framework. MUDA is a new infrastructure of the National
56 Institute of Geophysics and Volcanology (INGV, www.ingv.it) devoted to archive daily and distribute
57 quasi real time geophysical and geochemical multiparametric data recorded in continuous or near-
58 continuous mode at selected sites installed at the most tectonically active Italian areas (Figure 2).
59 MUDA was designed in the framework of INGV Dynamic Planet S2-project (i.e. 3D structure of Italy
60 from multidata analysis. Passive/active seismic, magnetic, magnetotelluric, electrical, gravimetric
61 prospecting, <https://progetti.ingv.it/it/pian-din>) and its development is ongoing in the framework of
62 the INGV Dynamic Planet GEMME project (Integrated Geological, gEophysical and geocheMical
63 approaches for 3D Modelling of complex seismic site Effects).

64 The need for an infrastructure capable of acquiring, storing, organising and publishing
65 multiparameter data in near real time arose following the installation of the Garda multiparameter
66 seismic network, PDnet (<https://eida.ingv.it/it/networks/network/ZO>), installed starting from 2021 as
67 part of the Task-S2 of the INGV Dynamic Planet project (Massa et al., 2021; Ferrari et al., 2024). In
68 this framework, MUDA collects information from different types of sensors, such as seismometers,
69 accelerometers, hydrogeochemical for physical-chemical parameters in waters, geochemical for
70 measuring the diffusive flux of carbon dioxide (CO₂) from the soil or detecting the air Radon
71 concentration, and meteorological stations. The aim is to constraint the influence due to exogenous
72 parameters in order to make potential correlations between seismic phenomena and variations
73 concerning monitored parameters (i.e. groundwater level, temperature, electrical conductivity, CO₂
74 soil flux, air Radon concentration; Barberio et al., 2017; Chiodini et al., 2020; Mastrotillo et al.,
75 2020).

76 The challenge of MUDA is to provide the end-user a high quality dynamic but also
77 simultaneous and continuous monitoring of groundwater physical parameters, meteorological data
78 and seismic signals, together with gas concentration such as Radon or soil CO₂-CH₄ fluxes (Figure
79 3). In order to furnish the main information for a detailed interpretation of local phenomena in the
80 framework of multi-hazard assessment, the multiparametric data are provided together with all
81 necessary stations and sites metadata, supplied with a complete geological and morphological
82 description (Figure 4).

83

84 **2 Seismotectonic framework and seismicity**

85

86 The multiparametric sites now included in MUDA are located in five main target areas (Figure
87 2): Lake Garda, eastern Alps, Po alluvial basin, Northern and Central Apennine chains (Table 1).
88 Concerning instrumental seismicity (<http://terremoti.ingv.it/>), in the last 40 years, thousands of small
89 to moderate energy seismic events (Figure 2) occurred in Northern Italy. Despite the low-to-medium
90 seismic hazard of the area (Stucchi et al., 2011), the high level of exposure (e.g. metropolitan areas,
91 industrial plants etc.), the local geological condition and the proximity of active buried seismogenic
92 structure (Burrato et al., 2012) make many portions of North Italy a medium to high seismic risk zone
93 (Massa et al., 2022b, Lai et al., 2020).

94 In particular, the Garda region (Area 1, Figure 2) is characterized by low-to-moderate
95 seismicity with the active tectonic regime located on the margin of the southern Alpine chain
96 controlled by the Africa-Europe convergence. The main active faults affecting the area consist of
97 mainly NNE-SSW trending thrusts (Galadini et al., 2001). For instance, the November 24, 2004,
98 Vobarno M_w 4.8 earthquake (<https://terremoti.ingv.it/event/1564989>), generated maximum
99 macroseismic intensities (I_{max}) of VII/VIII (<https://emidius.mi.ingv.it/CPTI15-DBMI15/>, Locati et
100 al., 2022). It is worth noting that in the past the same area was struck by several powerful events, such

101 as the October 30, 1901, Salò $M_w=5.4$ earthquake (<https://emidius.mi.ingv.it/CPTI15-DBMI15/>,
102 Rovida et al., 2022).

103 Moving eastwards (Area 2, Figure 2), the highest rate of energetic events in Northern Italy is
104 associated to the South-verging thrust faults typical of the central and East South Alpine Chain
105 (Battaglia et al., 2004; Serpelloni et al., 2005; D'Agostino et al., 2008), due to the North-South
106 convergence between the Adriatic microplate and the Alps. The most recent destructive earthquake
107 occurred in Friuli, during the seismic sequence of May 6, 1976, with $M_w= 6.5$ (Pondrelli et al., 1999
108 and reference therein), whereas the largest historical event was the 1695 Asolo earthquake, with an
109 estimated $M_w=6.48$ (<https://emidius.mi.ingv.it/CPTI15-DBMI15/>) broadly associated to the thrust
110 system of the Montello area (Danesi et al., 2015).

111 South of the Alps, the Po alluvial plain (Area 3, Figure 2) represents a very deep foreland
112 basin of two opposing verging fold-and-thrust belts developing in the framework of the African and
113 European plates relative convergence (Pieri and Groppi, 1981; Bigi et al., 1990). Despite the flat
114 morphology, the Po plain is far from being an undeformed domain, since the outermost and most
115 recent thrust fronts of the two belts are buried by the Plio-Quaternary sedimentary sequence (Burrato
116 et al., 2012). The historical and instrumental Italian seismic catalogues show that the southern Po
117 plain is affected by low to moderate seismicity, with M_w up to 5.8 during the 2012 sequence (Luzi et
118 al., 2013). Considering the historical seismicity (Rovida et al., 2020), the central part of the Po plain
119 was struck by the more significant North Italy earthquake on January 3, 1117, with an estimated
120 $M_w=6.52$.

121 Moving southwards, the Northern Apennines (Area 4, Figure 2) underwent the regional
122 seismicity associated with the Apennine fronts defined by different arcs of blind, North-verging
123 thrusts and folds (Mazzoli et al., 2015; Chiaraluce et al., 2017), capable of generating moderate
124 energetic seismic events with a maximum magnitude around 6 (i.e. June 5, 1501, $M_w 6.05$, Rovida et
125 al., 2022). In particular, this area hosts the Nirano site (Table 1), in the Regional Natural Reserve of
126 Salse di Nirano (Giambastiani et al., 2024; Romano et al., 2023), an area lying upon an anticline

127 structure of the North-East verging fold-and-thrust Apennine belt characterized by one of the largest
128 mud volcano fields in Europe (Bonini, 2008; Castaldini et al., 2005) coupled to the emission of CH₄-
129 dominated gases (e.g., Buttitta et al., 2020).

130 Finally, two stations included in MUDA, are installed in the surroundings of the Norcia
131 alluvial basin (Area 5, Figure 2), an area characterized by high seismic hazard and seismicity rate due
132 to dense extensional NW-SE active fault systems (e.g. Galadini et al., 1999, Brozzetti and Lavecchia,
133 1994) capable of generating high-magnitude earthquakes (Galli et al., 2018; 2019), such as the
134 January 14, 1703, M_w=6.9, earthquake or other moderate events such as the 1328, M_w=6.3, the 1730,
135 M_w=5.9, the 1859, M_w=5.5 and the 1979, M_w=5.8, earthquakes (Rovida et al, 2022). The recent
136 instrumental seismicity highlights the two main events occurring on August 24, 2016 and on the
137 October 30, 2016, with M_w 6.0 and 6.5 respectively, in an area a few kilometres of the Norcia plain
138 (e.g. Improta et al., 2019 and reference therein).

139

140 **3 State of the art**

141

142 At present, in Italy and Europe, the seismological communities in general are fairly advanced
143 in their running of both network data management and seismic data sharing. In Italy, the main seismic
144 network is represented by the National Seismic Network (RSN,
145 <https://eida.ingv.it/it/networks/network/IV>, Margheriti et al., 2020), managed by INGV and
146 sometimes integrated for real time data exchange by many local or regional networks (Massa et al.,
147 2022). The RSN permanent network is codified through the IV code assigned by the International
148 Federation of Digital Seismograph Networks, FDSN (<https://www.fdsn.org/>). The RSN station codes
149 are registered at International Seismological Center, ISC (<http://www.isc.ac.uk/>), while data, recorded
150 following the SEED (Standard for the Exchange of Earthquake Data,
151 http://www.fdsn.org/seed_manual/SEEDManual_V2.4.pdf) format, are shared (Danacek et al., 2022)
152 through the EIDA-Italia node (European Integrated Data Archive, <https://eida.ingv.it/it/>). In Italy,

153 INGV provides many websites and thematic databases for real time data quality and distribution,
154 such as EIDA-Italia, ISMDq (INGV Strong Motion Data quality, <https://ismd.mi.ingv.it> , Massa et
155 al., 2022), ITACA (ITalian Accelerometric Archive, <https://itaca.mi.ingv.it>, Pacor et al., 2011), ESM
156 (Engineering Strong Motion database, <https://esm-db.eu/>, Luzi et al., 2016), BSI (Italian Seismic
157 Bulletin, <https://terremoti.ingv.it/bsi>, Marchetti et al., 2016), TDMT (Time Domain Moment Tensor,
158 <https://terremoti.ingv.it/tdmt>, Scognamiglio et al., 2009), ShakeMaps (<https://shakemap.ingv.it/>,
159 Michelini et al., 2020), etc.

160 Differently, the geochemical community has still not developed a so capillary network of automatic
161 stations for data acquisition, management and sharing, as the seismic community does. This mostly
162 depends on the fact that only a few geochemical parameters/tracers can be measured directly in the
163 field and in near real-time [e.g., diffusive flux of CO₂ from the soil through accumulation chamber
164 method (Chiodini et al., 1998; Carapezza et al., 2004; Inguaggiato et al., 2011a; Rizzo et al., 2015),
165 Radon concentration in atmosphere or from the soil with specific Geiger counters, concentration of
166 H₂O, CO₂, SO₂, H₂S, CH₄, halogens in atmosphere through MULTIGAS sensors (Aiuppa et al., 2005;
167 Shinohara et al., 2005) or FTIR technique (e.g., Allard et al., 2005), SO₂ flux in atmosphere by DOAS
168 and UV techniques (Burton et al., 2009; Aiuppa et al., 2021)]. It must be also highlighted that most
169 of the automatic measurements of geochemical parameters above reported were developed and
170 applied in volcano monitoring, while only recently the geochemical community is moving to apply
171 some of those tracers to seismic monitoring. In terms of hydrogeochemical monitoring, apart the
172 physical-chemical parameters in water (e.g., temperature, water level, electric conductivity, and
173 others such as pH and Eh but with less precision and accuracy) for which automatic sensors exist
174 since long time, the automatic and high-frequency measurement of the water's composition is limited
175 to a few sensors developed in the last decade or so, which mostly focus on the concentration of a few
176 gas species dissolved in waters (e.g., CO₂, CH₄, total gas pressure; De Gregorio et al., 2005,
177 Inguaggiato et al., 2011b). As for gas sensors, most of the automatic measurements of water's
178 composition were developed for volcano monitoring applications.

179 At present, in Italy, hydrogeochemical and geochemical seismic monitoring is limited to
180 selected areas or sites, and it is essentially performed by several departments of INGV in the
181 framework of individual initiative such as the Alto Tiberina Near Fault Observatory (TABOO,
182 <https://ingv.it/en/monitoring-and-infrastructure-a/monitoring-networks/the-ingv-and-its->
183 [networks/taboo](https://ingv.it/en/monitoring-and-infrastructure-a/monitoring-networks/the-ingv-and-its-networks/taboo), Chiaraluce et al., 2014) or recent and on-going INGV projects such as the Dynamic
184 Planet (<https://progetti.ingv.it/it/pian-din>), FURTHER (<https://progetti.ingv.it/en/further>), MYBURP
185 ([https://progetti.ingv.it/it/pian-din#myburp-modulation-of-hydrology-on-stress-buildup-on-the-](https://progetti.ingv.it/it/pian-din#myburp-modulation-of-hydrology-on-stress-buildup-on-the-irpinia-fault)
186 [irpinia-fault](https://progetti.ingv.it/it/pian-din#myburp-modulation-of-hydrology-on-stress-buildup-on-the-irpinia-fault)), Multiparametric Networks or Rebuilding Central Italy, DL50 and related tasks (e.g.
187 Idro-DEEP CO₂, Idro-Calabria, Idro-Nord), concerning the groundwater continuous monitoring (e.g.
188 springs and thermal waters) of different areas of mainly Central and Southern Italian Apennines
189 (<https://www.pa.ingv.it/index.php/progetti/>) and Radon monitoring (IRON project,
190 <https://ingv.it/monitoraggio-e-infrastrutture/reti-di-monitoraggio/l-ingv-e-le-sue-reti/iron>). In
191 particular, the Alto Tiberina Near Fault Observatory is managed by EPOS (European Plate Observing
192 System) research infrastructure (<https://www.epos-eu.org/>) of which the mission is to foster the
193 integration of solid earth data and their by-products made by the entire European scientific
194 community: in this case, seismological, geophysical, geodetic and geochemical data recorded by
195 TABOO-Near Fault Observatory are accessible via the FRIDGE European web portal
196 (<https://fridge.ingv.it/index.php>).

197 Further local monitoring initiatives are provided by other institutions or Universities through
198 the installation of geochemical stations and probes in different parts of the national territory such as
199 in Tuscany, by the IGG-CNR (Institute of Geoscience and Earth Resources,
200 <https://www.igg.cnr.it/en>), in Southern Italy, by the IMAA CNR (Institute of methodologies for
201 environmental analysis, [https://www.cnr.it/en/institute/055/institute-of-methodologies-for-](https://www.cnr.it/en/institute/055/institute-of-methodologies-for-environmental-analysis-ima)
202 [environmental-analysis-ima](https://www.cnr.it/en/institute/055/institute-of-methodologies-for-environmental-analysis-ima)) or Central Italy, by the Earth Sciences Department (DES,
203 <https://www.dst.uniroma1.it/en>) of Sapienza University of Rome (Martinelli et al., 2021).

204 Consequently, at a national scale the hydrogeochemical and geochemical monitoring is not
205 organized by using an ad hoc reference institutional database or web portal able to homogeneously
206 archive and distribute high quality multiparametric data to the scientific community. At present and
207 at the best of our knowledge, the only existent databases focus only on mapping gas emissions (e.g.,
208 MaGa, <http://www.magadb.net/>) or thermal springs, without archiving data from a regular
209 monitoring. A first attempt was recently made in the framework of an agreement between the National
210 Institute of Geophysics and Volcanology (INGV) and the National System for Environmental
211 Protection (SNPA, <https://www.snambiente.it/>, comprising the Regional Environmental Protection
212 Agencies, ARPA, and the Italian Institute for Environmental Protection and Research, ISPRA,
213 <https://www.isprambiente.gov.it/>), with the aim of sharing data from the continuous monitoring of
214 water wells and springs, in particular the piezometric level, temperature, electrical conductivity,
215 salinity and total dissolved solids (Comerci et al., 2019).

216

217 **4 MUDA database**

218

219 MUDA is a dynamic and relational multiparametric database designed and built using a table
220 structure that can correlate data of a different nature (i.e. seismic, hydrogeochemical, geochemical,
221 meteorological). It is adaptable to further types of data from other projects and capable of integrating
222 perfectly with those already acquired via both real time and off-line transmission vectors (Figure 5).
223 The MUDA database is based on MySQL (<https://www.mysql.com/it/>), a popular and efficient open-
224 source relational database management system for handling large amounts of data. Particular attention
225 has been paid to optimising and, above all, integrating all the different types of data taken from
226 different sources while trying to maintain a certain structural uniformity, also open to possible future
227 new implementation.

228 Data collection takes place separately for each type of monitoring station (Table 1), each according
229 to its preferred channels (email, ftp system, Application Programming Interface API, Structured

230 Query Language SQL) with the effort to improve each procedure, avoid data loss and minimise the
231 time taken to receive data.

232 Data are acquired and then archived on a centralised server from which all pre-processing procedures
233 are then carried out to insert this data, after appropriate checks and automatic analysis, into the MUDA
234 database (see next chapter for details). All data downloaded from the remote stations, after the check
235 and processing phase are stored in files before the population of the MySQL database. This is also
236 convenient to have a native and complete data backup, for future requirements.

237 The MUDA database is structured to consider all the different types of monitoring stations at the same
238 multiparametric site through a univocal internal site code, linked to all different types of data. At the
239 same time, however, the independence of the data of each different station is also maintained, as each
240 individual site may have its own particular condition and metadata. For each type of monitoring
241 station, the MUDA database includes 2 tables, one for the station metadata and the other for the
242 recorded data, linked by a unique station id.

243

244 **4.1 Processing of raw data**

245

246 The MUDA project currently includes 5 types of data: hydrogeochemical, meteorological,
247 Radon, CO₂ and seismic. All data are pre-processed to align each time series to the common UTC
248 (Coordinated Universal Time) time. Hydrogeochemical, seismic, meteorological and Radon data are
249 moreover resampled in order to have a representative data each few minutes (i.e. from 1 to 5), namely
250 a good enough interval to see possible cross-correlation signals on different parameters. A data
251 resample is a priori necessary in order to, at first, homogenize data for viewing and comparison, but
252 also to allow the web page to have a fast response to any query involving long time periods (actually
253 up to a maximum of 30 days) of continuous and high frequency multiparametric recordings. In
254 particular, while hydrogeochemical, gas and meteorological data are uploaded into MUDA database
255 as raw data with only a consistency check, the seismic data are pre-processed in order to obtain

256 waveforms metadata to be included into MUDA database and to be easily comparable in terms of
257 time series to the other parameters.

258 The processing of raw data for each of the 5 parameters included in MUDA is described in detail in
259 the following.

260

261 The hydrogeochemical data are acquired by two different types of instrumentation, the first
262 provided by Van Essen Instruments (<https://www.vanessen.com/>) and the second by STS-Italia S.r.l.
263 (<https://www.sts-italia.it/>). Data recorded by Van Essen Instruments and STS-Italia are set to sample
264 records every one and ten minutes, respectively. In both cases, groundwater level (m), electrical
265 conductivity ($\mu\text{S}/\text{cm}$), and temperature ($^{\circ}\text{C}$) are achieved using probes (e.g. CTD-Diver®,
266 <https://www.vanessen.com/>) installed in correspondence of wells or springs by using weir
267 flowmeters; the recorded chemical and physical parameters are sent at defined time intervals to the
268 remote company head offices and then to the INGV acquisition centre by proprietary API or email.
269 At present, remote stations send data in ASCII format twice a day (i.e. 9 a.m. and 9 p.m., Central
270 European Time, CET) as an email attachment or by ftp-protocol. Depending on the target
271 instrumentation, before populating the MUDA database, a pre-processing is necessary: as an example,
272 the Van Essen probes for water wells need a barometric compensation to account for atmospheric
273 pressure variations in order to provide the corrected water level value (Ferrari et al., 2024). Automatic
274 data acquiring and processing tools have been developed in Python (<https://www.python.org/>), while
275 automatic tools for populating the MUDA database have been developed in PHP language
276 (<https://www.php.net>).

277

278 The meteorological data included in MUDA are provided by Davis Vantage Vue®
279 instrumentation (<https://www.davisinstruments.com/>). Each single meteorological station, placed
280 near the water well, provides information on atmospheric pressure (mbar), temperature ($^{\circ}\text{C}$), humidity
281 (%), rainfall amount (mm), wind speed and direction. Also in this case, data take advantage of

282 GPRS/LTE technologies and are gathered by a dedicated WeatherLink Live cloud platform, making
283 them available in real time on the dedicated website (<https://www.weatherlink.com/>). With samples
284 every one minute, data are archived into the Davis server-cloud and then shared by payment to the
285 end-users (e.g. INGV server) through proprietary Application Programming Interface (API) set into
286 an automated ad-hoc developed python tool, suited for all the different kinds of meteorological
287 instrumentation at each site. Just as for hydrogeochemical data, meteorological parameters are then
288 automatically inserted into the MUDA database twice a day (i.e. 9 a.m. and 9 p.m. CET) using a
289 procedure developed in PHP.

290

291 The Radon data are provided by the IRON network (Italian Radon mOnitoring Network,
292 <https://ingv.it/monitoraggio-e-infrastrutture/reti-di-monitoraggio/l-ingv-e-le-sue-reti/iron>, Cannelli
293 et al., 2018). Stations, placed next to the water well, measure the concentration of gas in the air using
294 a photodiode detector (AER Plus, Algade), with a sensitivity of 15 Bq/m³ by counts/hour. Data are
295 measured and acquired every 4 hours together with temperature and humidity, Radon data are
296 transmitted in real time by the Sigfox (<https://www.sigfox.com>) 0G-technology and archived at the
297 Sigfox cloud, with the exception of particularly remote sites where a periodic local data downloading
298 is also necessary. Radon data are provided in csv format, where the concentration is measured in
299 Bq/m³, and then uploaded into the MUDA database using an ad-hoc developed PHP tool. In this case,
300 the procedure is manually started after each single data downloading.

301

302 The CO₂ soil flux measurements are acquired using an accumulation chamber provided by
303 Thearen S.r.l (<https://thearen.com/>). The permanent stations have a no-stationary flux chamber and
304 are equipped with an infrared analyser measuring CO₂ concentrations (g·m⁻²·d⁻¹) in a time frame of
305 three minutes. A single CO₂ flux measure is returned each hour already corrected for pressure (mbar)
306 and temperature (C°) recorded inside the chamber. Soil temperature and humidity (%) and
307 meteorological parameters (atmospheric pressure, temperature, humidity, rain, wind speed and

308 direction) are acquired concurrently. Data are sent to the head company server-cloud through a
309 dedicated modem with automatic data transmission. Data are acquired daily by the INGV acquisition
310 centre through an ad-hoc server to server link using an internal INGV-VPN (Virtual Private Network)
311 connection. Data provided in csv format, are then daily automatically inserted into the MUDA
312 database by using an ad-hoc developed PHP tool.

313

314 The Seismic data are acquired by selected stations of the Italian National Seismic Network
315 (RSN, <https://eida.ingv.it/it/networks/network/IV>) and the multiparametric network of Northern Italy
316 (PDnet, <https://eida.ingv.it/it/networks/network/ZO>) placed near the water well used for
317 hydrogeochemical data. Recorded data are codified following the international standard commonly
318 used by the seismological community, namely the FDSN (<https://www.fdsn.org/>) network-station
319 code and SEED (Standard for the Exchange of Earthquake Data, http://www.fdsn.org/seed_manual/SEEDManual_V2.4.pdf) format supported by European
320 Integrated Data Archive, EIDA (<https://eida.ingv.it/it/>) and maintained by the FDSN. Data are
321 transmitted by different technologies (LTE, satellite, etc.) to the INGV Milano acquisition centre
322 where they are archived through a Seiscomp4 (<https://www.seiscomp.de/doc/apps/seedlink.html>)
323 client to improve the SeedLink real time data acquisition protocol. Data are archived in the standard
324 binary miniSEED format (<http://ds.iris.edu/ds/nodes/dmc/data/formats/miniseed>) and organized in a
325 structured archive. Seismic data are pre-processed every night considering the 24 hours of all
326 miniSEED files recorded by stations on the previous day and then checked for quality before being
327 automatically included in the MUDA database by using an ad-hoc developed PHP tool.

329 In dependence of the adopted sampling rate (i.e. 100 Hz for seismometers and 200 Hz for
330 accelerometers) the amount of continuous data stream per day, relative to a single channel at each
331 single station, ranges between 6 and 10 Mbyte for seismometers and between 15 and 20 Mbyte for
332 accelerometers. Considering many seismic stations, the result is a total daily archive in the order of
333 Gigabytes, not easy to organize in the framework of a quasi-real time data distribution provided by a

334 thematic web portal. In this framework, also considering the sampling rate of the other
335 multiparametric instrumentation (i.e. spanning from one record per minute to one record every four
336 hours), the continuous seismic data streams are processed in order to conform the contents to the web
337 portal requirements before inclusion in the MUDA database. In particular, every night at 2 a.m.
338 miniSEED files relative to the 24-hour recordings of the previous day are selected at each station and
339 processed by using an ad-hoc procedure developed by merging the Bash and SAC (Seismic Analysis
340 Code, <https://ds.iris.edu/files/sac-manual/>) scripting languages.

341 The processing scheme starts by downloading at each single recording station 24 hours of miniSEED
342 files; data are then separated into 288 sub-windows, each one with length of 5 minutes starting from
343 the origin time of each single miniSEED file (usually corresponding to the 00:00:00 UTC if the station
344 works well). Then, for each 5-minute windows, raw data recorded in counts are converted to the
345 proper unit of measurements (cm/s for seismometers and gal for accelerometers) and the sensor
346 response curves are removed by deconvolution and finally filtered using a 4th order Butterworth filter
347 in the range 0.1 - 20 Hz. For each single sub-window relative to a specific channel recorded by a
348 specific station, the RMS (Root Mean Square, e.g. Goldstain et al., 2003), the maximum ground
349 shaking in terms of velocity (cm/s), the mean amplitude value of the whole FFT (cm/s/Hz) (Fast
350 Fourier Transform, e.g. Bormann 2012) and the maximum amplitude of the FFT for frequency
351 interval spanning from 0.1 Hz to 20 Hz, are calculated, providing for each parameter 288 values per
352 day, corresponding to the daily upload of hydrogeochemical and meteorological data. In particular,
353 the RMS is calculated for the entire time windows using the following equation:

354

$$355 \quad x_{RMS} = \sqrt{[1/n (x1^2 + x2^2 + \dots + xn^2)]} \quad (1)$$

356

357 where x is the amplitude of the single sample, and n the number of samples of the trace considered.
358 Daily time series of RMS, PGV, FFT-mean and FFT(f) are finally uploaded into the MUDA database
359 using an ad-hoc developed PHP tool.

360
361
362 **4.2 Data availability and dissemination**

363

364 MUDA publishes and shares the available data recorded at each site through a specific web
365 interface developed in PHP (<https://www.php.net/>) to easily and effectively interact with MUDA SQL
366 database, and using a responsive design in HTML5, capable of adapting automatically to any device
367 on which it is displayed (i.e. PC, tablet, smartphone, etc.). As a final step, the data publication required
368 assigning a regular DOI associated to the DB and provided by INGV data management office through
369 a standard procedure. The final DOI of MUDA is <https://doi.org/10.13127/SD/ku7Xm12Yy9>. Data
370 have been licensed using the Creative Commons License CC BY 4.0. MUDA web portal publishes
371 multiparameter data daily and updated to the previous day. It offers the chance to view and download
372 dynamic time series for all available data and for different time periods, up to a maximum of 30 days.
373 In reference to longer periods, an e-mail request can be sent to: muda@ingv.it.

374 The web portal has a main page showing an interactive map of Northern and Central Italy, as
375 at present MUDA acquires data from automatic stations located in this part of the Country, where the
376 multiparametric stations are indicated by triangles with pop-ups showing the main features (i.e.
377 coordinates and available instrumentation) of the target site, including the direct access to the dynamic
378 data viewing (Figure 3) and to the single station page (Figure 4). The home page on the top right
379 corner shows a pop-up menu with selectable thematic layers including the reference seismic hazard
380 map of the national territory in terms of peak ground acceleration (MPS04 working group,
381 <http://zonesismiche.mi.ingv.it/>, Stucchi et al., 2011), the seismogenic areas and the active faults taken
382 from the Database of Individual Seismogenic Sources database (DISS, <https://diss.ingv.it/>, DISS
383 working group 2021), recent (<https://terremoti.ingv.it/>) and historical
384 (<https://emidius.mi.ingv.it/CPTI15-DBMI15/>) seismicity bulletins, and the location of seismic
385 stations of the National Seismic Network (RSN, <https://eida.ingv.it/it/networks/network/IV>) managed
386 by INGV.

387 The *View & Download DATA* web page, accessible from the horizontal tool bar of the home
388 page, opens the dynamic data viewing (Figure 3). Users can select for each multiparameter site the
389 time series to be displayed backwards in time (i.e. 1 day, 7 days, 15 days, 30 days) starting from a
390 selected date. Once the site and period have been chosen, the available data automatically appear
391 synchronised with respect to UTC (Coordinated Universal Time). From top to bottom, these are:
392 hydrogeochemical data from well or spring sensors showing water temperature (°C), electrical
393 conductivity ($\mu\text{S}/\text{cm}$) and the value of the water column (m) above the sensors; meteorological data
394 showing air temperature (°C) and rainfall (mm); seismometric data showing the RMS, the maximum
395 ground velocity values (cm/s), the average FFT amplitude values, the Fourier spectrum values for
396 frequency bands selected in the interval 0.1 - 20 Hz; Radon gas emissions (Bq/m^3) and soil CO_2 flux
397 ($\text{g}\cdot\text{m}^{-2}\cdot\text{d}^{-1}$). All interactive graphs can be zoomed with the left mouse button and they enable selecting
398 individual functions using pop-up layers. In each graph, in the top right-hand corner, it is possible to
399 view the individual image in full screen and download the selected data in csv (Comma Separated
400 Values) format as well as the images in pdf (Portable Document Format), png (Portable Network
401 Graphic), jpeg (Joint Photographic Experts Group), svg (Scalable Vector Graphics) formats. The last
402 selectable item, on the right of this page, gives the possibility of viewing a single parameter, for a
403 more detailed observation.

404 A further topic of the MUDA web portal is the single station web page (i.e. link *STATIONS*),
405 also reachable from the horizontal tool bar. This web page is designed to provide a first and general
406 geophysical and geochemical characterization of each multiparametric site. In particular, each single
407 station web page shows, on the left, a thematic map indicating the location of the monitoring site.
408 Below the map, the two links provide a geological and morphological setting of the area. For each
409 recording site, a portion selected from the geological map at a 1:100,000 scale (Società Geologica
410 Italiana, <http://www.isprambiente.gov.it/it/cartografia/>) is provided, with topographic base at
411 1:25,000 scale (Istituto Geografico Militare,
412 http://www.igmi.org/prodotti/cartografia/carte_topografiche/). Concerning morphology, for each

413 recording site, a topographic map (i.e. Slope and Ridge) is proposed by considering the available
414 digital elevation model (ASTER GDEM with a cell size of 10 m,
415 <https://www.earthdata.nasa.gov/news/new-aster-gdem>). Starting from the processed DEM, the slope
416 map was constructed with three topographic classes (0° – 15° , 15° – 30° , and $>30^{\circ}$), considering the
417 break values defined in the current Italian seismic code (NTC, 2018). The ridgelines were extracted
418 using the Topographic Position Index (TPI) algorithm (Weiss, 2001; Pessina and Fiorini, 2014). On
419 the right, the web page shows thematic tables relative to the installed instrumentation. At each site,
420 besides the general information on coordinates and technical features of the instruments, a
421 geophysical characterization of the site is also provided in terms of polarized horizontal to vertical
422 spectral ratio (HVSR) on ambient noise (Nakamura, 1989) and each single log performed in the wells
423 regarding water electrical conductivity and temperature as a function of the available stratigraphy
424 together with the main features of monitored well or spring. Finally, in each station web page, graphs
425 relative to the whole hydrogeochemical time series are also downloadable.

426

427 **5 Data Records**

428

429 At present (i.e. March 31, 2024), MUDA includes data from 25 multiparametric sites (Table
430 1) located in Northern and Central Italy (Figure 2), both already monitored by permanent INGV
431 infrastructures or installed in the framework of recent INGV research projects. It is worth mentioning
432 that not all multiparametric sites are characterized by homogeneous multiparametric instrumentation
433 (Figure 6). In any case, all available data are always sent in real time to the INGV acquisition centres.
434 In particular, concerning seismic data, the multiparametric sites include 7 stations belonging to the
435 permanent National Seismic Network (RSN, <https://eida.ingv.it/it/networks/network/IV>) and 12
436 stations belonging to the temporary multiparametric network of Northern Italy (PDnet, FDSN code
437 ZO, <https://eida.ingv.it/it/networks/network/ZO>), installed in the framework of the INGV Dynamic
438 Planet S2-project. These sites are located in Northern Italy, around the Lake Garda, at the southern

439 limit of the Eastern Italian Alps and in the central portion of the Po Plain (Figure 2). Two further
440 seismic stations (PDN11, PDN12, table 1) have recently been installed in the framework of the INGV
441 Dynamic Planet GEMME (Integrated Geological, gEophysical and geocheMical approaches for 3D
442 Modelling of complex seismic site Effects) project, in Norcia basin (Apennine chain in central Italy)
443 and its surroundings (Figure 2). Finally, one seismic station (PDN10, table 1) has been installed in
444 cooperation with the Dynamic Planet PROMUD (Definition of a multidisciplinary monitoring
445 PROtocol for MUD volcanoes) project, in the Salse di Nirano Reserve (Italian Northern Apennines,
446 Figure 2). In general, seismic stations are equipped with high dynamic 24-bit digital recording
447 systems coupled to enlarged (5s owner period) or broadband (120s owner period) seismometers. In
448 particular, at Oppeano multiparametric site (Table 1), borehole instrumentation is installed at 150 m
449 depth. Even if in some cases accelerometer sensors are coupled to the target seismometer
450 (velocimeter), MUDA includes only seismometric data due to their higher sensitivity and best
451 resolution with respect to possible occurrences of natural phenomena such as micro seismicity, local
452 weak motion earthquake occurrences and/or teleseisms or environmental modifications (i.e.
453 landslides, low atmospheric pressure, tides etc.).

454 Hydrogeochemical data are recorded in all 25 multiparametric sites (Table 1), at both wells
455 and springs set up in the framework of INGV Dynamic Planet projects (S2 and GEMME) and INGV
456 Multiparametric Networks or the Rebuilt central Italy, DL50 project. The Toppo site (Table 1),
457 installed in the eastern Alps in the framework of the Eccsel Eric consortium
458 (<https://www.eccsel.org/>), is managed by OGS (National Institute of Oceanography and Applied
459 geophysics, <https://www.ogs.it/en>) in cooperation with the University of Ferrara (Department of
460 Physics and Earth Science, <http://fst.unife.it/en>) and the INGV. At present, data included in MUDA
461 are recorded at 22 wells and 3 springs (Recoaro, Recoaro1, Feltre, see table 2). In general, wells have
462 depths ranging from a few meters (< 10 m) to a maximum of 300 m for Toppo and Mirandola sites
463 (Table 2). The instrumented wells have a mean depth between 5 and 150 m. Monitored sites are
464 mainly characterized by cold waters whose average temperatures range from 10.3 to 17.4 °C, except

465 for TRIPONZO site that owns thermal water (~ 30 °C; Table 2). A wide variety of water electrical
466 conductivity values (~ 130-88000 µS/cm; Table 2) are illustrative of heterogeneous compositions and
467 salt contents. Information on the presence of borehole pump (Table 2), frequency and intensity of
468 water pumping were carefully collected from well owners. Water level, temperature and electrical
469 conductivity changes are observed because of pumping for water chemical analysis (e.g., Balconi) or
470 irrigation purposes (e.g., Norcia) or functioning of spa (e.g., Triponzo). These anthropogenic
471 variations must be accounted for when analysing groundwater data. A comprehensive example of
472 data-processing able to recognize in groundwater time series both natural phenomena and
473 anthropogenic noise signals is reported in Ferrari et al. (2024) for the site of Balconi.

474

475 All sites monitored by hydrogeochemical instrumentation are also equipped with a
476 meteorological station able to capture the main atmospheric variations. Four sites (i.e. Montelungo,
477 Bondo, Norcia, Triponzo, table 1) are currently equipped with instrumentation able to record the
478 Radon concentration in the air. Sensors for Radon monitoring are part of the IRON network (Italian
479 Radon mOnitoring Network, [https://ingv.it/monitoraggio-e-infrastrutture/reti-di-monitoraggio/l-
480 ingv-e-le-sue-reti/iron](https://ingv.it/monitoraggio-e-infrastrutture/reti-di-monitoraggio/l-
480 ingv-e-le-sue-reti/iron)) of INGV. Finally, just one site (i.e. Nirano, table 1) is equipped with
481 instrumentation for Carbon Dioxide (CO₂) soil flux measurements.

482

483 In general, the multiparametric sites show co-located instrumentation, with a few exceptions
484 due to logistic difficulties during the site installation or other technical problems (e.g. sites with a
485 very high level of background seismic ambient noise or working pump installed in well). In all cases,
486 the reference seismic station is installed in the same geological, morphological and hydrogeological
487 context as the other instruments, possibly co-located or at least in the proximity. Hydrogeochemical
488 stations installed in a narrow area (e.g., Bulgarelli, Medolla, Mirandola and Secchia sites, table 2)
489 might refer to the same seismic station.

490

491 5.1 Data quality check

492

493 In order to verify the completeness and correctness of the recorded data, we carried out several
494 checks.

495 Concerning seismic data included in MUDA, the results of the processing procedure to
496 produce 5 minutes interval data are verified to check the capacity of the proposed processing scheme
497 to represent a real marker to detect earthquakes or environmental phenomena. Figure 7 reports an
498 exhaustive example at the Oppeano site for events recorded by the seismic station on December 29,
499 2020. Figure 7 shows in the panel *a* (top) the occurrences of subsequent events in a narrow time
500 window spanning from 2020/12/29 14:02:40 to 15:36:57 UTC. The first evident transient is related
501 to the regional $M_w=6.3$ Croatia earthquake on 2020/12/29 at 12:19:54 UTC
502 (<https://terremoti.ingv.it/event/25870121>). A few hours later, a small sequence of three local weak
503 motion was recorded 12 km South West of Oppeano and localised by the INGV bulletin at 2020/12/19
504 14:02:40, 14:44:51 and 15:36:47 UTC with magnitudes of $M_L=3.4$, $M_L=2.8$ and $M_w=3.9$, respectively
505 (<https://terremoti.ingv.it/event/25871441>). In the bottom of panel *a* the results of our detector
506 procedure in terms of FFT interval is shown for the 288 data points of the 2020/12/29. It is evident
507 how all transients have been clearly recognized by marked peaks: in particular, the regional event,
508 occurring about 400 km East of the Oppeano well highlights a notable contribution at low frequency,
509 showing a clear peak for the FFT around 0.1 Hz. On the contrary, the local seismicity is well described
510 by peaks detected at higher frequency content, in particular ranging from 1 to 10 Hz. In this case, it
511 is worth noting how the high frequency content of FFTs also highlight variations in ambient noise
512 level between night and day. In the panel *b* of figure 7, the results of the detection procedure are
513 presented in terms of relative RMS, ground motion velocity and averaged FFTs (from top to bottom).

514 In order to publish reliable results, all continuous seismic data streams for all seismic stations
515 are checked daily for quality by the interoperability between MUDA and ISMDq (INGV Strong
516 Motion Data quality, <http://ismd.mi.ingv.it>, Massa et al., 2022). In this way all seismic stations

517 included in MUDA are checked for gaps (%), availability (%) and ambient noise level variation in
518 terms of PSD (Power Spectral Density) and PDF (Probability Density Function), in dB, as calculated
519 by McNamara and Buland (2004). Through ISMDq, it is possible to build temporal time series with
520 a maximum time length of up to 2 years for all stations included in MUDA in order to check at first
521 the correct functioning of the stations, the accuracy of used metadata, daily and seasonal variations
522 of ambient noise level and transient or permanent anthropic disturbances. In particular, in case of
523 failure in data transmission, the continuous monitoring of data gaps and availability allow us to
524 retrieve data directly from station memories thereby avoiding important gaps in the data.

525 Hydrogeochemical and geochemical data are checked daily for availability and gaps usually
526 due to a temporary lack of data transmission platforms (i.e. cellular line or satellite), in particular
527 during rainy and stormy days or more rarely due to malfunctioning of the instrumentation. In the first
528 case, the recorders, thanks to their internal memory and datalogging capacity, are able to archive data
529 up to a maximum of 30 days. If needed, the recovery of data is possible through a manual download.
530 Subsequently data are uploaded into the MUDA database by calling the same ad-hoc developed tools
531 for populating the database for each parameter, with appropriate flags. In some cases, water level time
532 series show unusual abrupt peaks (i.e. spurious spikes that are filtered) due to some problems during
533 the compensation of atmospheric pressure performed by the recording system in order to obtain the
534 correct values of water level: in general, misalignments in pressure compensation lead to wrong water
535 level values, usually with differences of ~ 10 m, as a consequence of the measured atmospheric
536 pressure usually around or slightly above 1000 mbar, considering that all the stations are within a few
537 hundred meters above sea level.

538 Other data included in MUDA (i.e. meteorological, Radon, CO₂ flux) do not need particular
539 processing. In any case, for all meteorological, Radon and CO₂ measurements, data are always
540 checked for gaps and possible spurious peaks that are deleted. In particular, meteorological data
541 regarding the pluviometry are archived and uploaded into MUDA as a single sample recorded each
542 minute, or even better, in some cases, at each individual movement of the rain gauge's tipping bucket

543 (0.2 mm every time). In these cases, before publishing the rain values on the web site, data are
544 cumulated in intervals of 1 hour directly in the SQL query made by the web portal, in order to better
545 highlight heavy storms or other particular meteorological phenomena.

546

547 **6 Multiparametric monitoring**

548

549 In this section, some examples of comparison among multiparametric data are presented and
550 discussed in the framework of their possible applications for research and services devoted to natural
551 hazard risk reduction.

552 An interesting example of multiparametric monitoring, concerning groundwater level
553 variation presumably related to large landslide phenomena has been collected at the Bondo (Table 1)
554 site and aquifer (Lake Garda area, Figure 2), where on the November 1, 2023, the water column above
555 the sensor in the well abruptly increased by ~ 20 m. This significant modification, also combined with
556 the diminishing temperature and electrical conductivity (Figure 8, panel *a*), happened
557 as a consequence of 2 days of intense rainfall with measured values of precipitation up to 400 mm in
558 a narrow area surrounding Bondo. It is important to highlight that the stratigraphy below Bondo is
559 mostly made of fractured-carsified limestones belonging to the Dolomia Principale formation (Upper
560 Triassic). To explain such a notable groundwater level variation, additional and contemporary natural
561 phenomena should be hypothesized; on the base of the information provided by the local media, in
562 the same period the area was affected by diffuse landslides. In particular, between October 31 and
563 November 1, 2023, a clear seismic transient (Figure 8, panel *b*) was recorded on all 3 components of
564 ZO.PDN3 station (Table 2), characterized by very long duration (i.e. some hours), higher amplitudes
565 with respect to the local ambient noise level (i.e. the Peak Ground Velocity, PGV was equal to 0.01
566 cm/s, comparable to a local earthquake with magnitude ranging from 2.5 and 3.0), prevalent high
567 frequency content (~ 5-30 Hz) and a strong polarisation with preferential amplification of motion
568 along the NS direction (Figure 8, panel *c*). In this case, the recorded transient at ZO.PDN3 could in

569 fact be attributable to local and diffuse landslides that could have modified the volume and/or the
570 extent of the aquifer and eventually the water flow infiltration and circulation through the rock
571 fractures by influencing the water level and leading the aquifer to be more sensitive to meteorological
572 events.

573 Meteorological events, in particular the intense rainfall period, also seem to have a strong
574 influence on Radon emission measurements, usually adopted as a possible marker in case of a tectonic
575 event. An example can be observed considering the complete Radon time series at the Bondo site
576 where data highlight a positive correlation with the seasonality, with increasing values in summer and
577 decreasing values in winter, following the trend of both atmospheric pressure and temperature. At
578 least during the monitored period, at the Bondo site no correlation with local seismicity appears to be
579 noticeable, while clear correlations between Radon outliers and the rainfall period are evident (Figure
580 9, panel *a*). It is worth mentioning how not all Radon sensors show the same behaviour with respect
581 to the season. At the Montelungo site (Table 1), for instance, data show a complete anti-correlation
582 with the seasons (Figure 9, panel *b*), with lower values in summer and higher values in winter,
583 probably as a consequence of the different local geological and morphological setting.

584 A further example regards the CO₂ flux variation, measured at the Nirano site (Table 1) in
585 October 2023 (Figure 10, panel *a*) during an intense period of weak motion earthquakes localized
586 very close to ZO.PDN10 station, installed in the area of the Salse di Nirano regional park. Starting
587 from June 2023, the area of Nirano showed an increase in the local seismicity. In the period
588 2023/06/01 to 2023/11/15, 32 earthquakes with local magnitude (M_L) in the range 2.0-3.5 were
589 recorded with a maximum epicentral distance from Nirano of 30 km. In particular, the strong events
590 with $M_L=3.5$ occurred on October 30, 2023 (04:25:53 UTC). Considering the CO₂ time series
591 recorded at Nirano and a time period spanning from October 15 to November 15, 2023, it is possible
592 to highlight the presence of many CO₂ data points with values exceeding the limit of +1 standard
593 deviation (Figure 10, panel *b*), with respect to the average values of the period. Many outliers were
594 recorded just before and also soon after the $M_L=3.5$ target earthquake. It worth noting that this

595 evidence should be carefully evaluated also considering other parameters (for instance, atmospheric
596 pressure, soil moisture and temperature), even though no relevant rainfall episodes occurred in that
597 period.

598 Further case studies concern the correlation between meteorological (i.e. temperature and
599 rainfall) and groundwater parameters. Understanding water level fluctuation patterns is one of the
600 pillars for designing adaptive management practices that can mitigate the impacts of extreme water
601 levels on infrastructure and associated economic activities (e.g. Gerten et al., 2013, Alley et al., 2002,
602 Taylor et al., 2009; Russo and Lall, 2017). Groundwater recharge is difficult to estimate, especially
603 in fractured aquifers, because of the spatial variability of the soil properties and because of the lack
604 of data at basin scale. A possible solution consists in inferring recharge directly from the observation
605 in boreholes (Guillaumot et al., 2022), even if the direct measures in wells overlook the impact of
606 lateral groundwater redistribution in the aquifer. When evaluating the effect of exogenous parameters
607 on groundwaters, rainfall is the main factor in promptly influencing all monitored groundwater
608 parameters (e.g. Mancini et al., 2022, Guillaumot et al., 2022), with a variable aquifer response with
609 respect comparable amounts of precipitation in the same period. Figure 11 shows an example of
610 groundwater recordings related to the meteorological event of October 2023 at Volargne and Fonte
611 sites (table 1). It is worth noting how in the first site (Figure 11, panel *a*) a gradual and moderate rise
612 in water level is contrasted by a faster and larger (less than 2 hours) increase in water level at the
613 Fonte site (Figure 11, panel *b*), which shows an intense influence of the rainfall, also proved by the
614 extremely variable temperature and conductivity records not observed in the other sites (Ferrari et al.,
615 2024). The light grey box in Figure 11 highlights another instant response of Fonte groundwater to
616 precipitation which is even more sharper than the one described above and also involves electrical
617 conductivity decrease and temperature increase.

618 The atmospheric temperature is moreover proven to affect groundwater temperature,
619 especially in aquifers down to ~ 20 m depth (e.g. Lee and Hahn, 2006, 2021; Taylor and Stefan, 2009;
620 Menberg et al., 2014). Monitoring sites having at least 1 year of recordings are taken into account to

621 analyse groundwater temperature seasonal oscillations and correlations to air temperature. In our
622 case, the absence of seasonality is detected at the Bondo, Montelungo and Volargne sites (Table 1)
623 where the constant groundwater temperatures could be explained by the aquifer depth (~ 50 m). In
624 other cases, such as the Casaglia site (Table 1), despite the depth of aquifer of a few meters below
625 ground level, the relevant water (~ 40 m) column above the hydrogeochemical sensor dampened
626 possible temperature fluctuations (Bucci et al., 2020; Egidio et al., 2022). On the contrary, at the
627 Balconi site (Table1), despite the aquifer depth is greater than 50 m, a nearly seasonal variation
628 characterized by maximum values reached in summer and minima in winter, is observed, in
629 agreement with the measured air temperature periodicity (Ferrari et al., 2024). However, it should be
630 evaluated whether this temperature variation in specific seasons is directly attributable to
631 meteorological reasons or to anthropogenic causes, due to intense irrigation occurring in the area of
632 Balconi during the most dry and hot months of the year.

633

634 **7 Usage Notes and conclusions**

635

636 The technical validation allowed us to obtain a reliable and homogenous dataset of continuous
637 multiparametric time series and associated metadata. For hydrogeochemical, meteorological, Radon
638 and CO₂, data are published in a raw format after a pre-processing whose main scope was just to
639 detect gaps and spurious peaks to be deleted from the time series. Seismic data are published after
640 applying a 5-minute resampling to the raw miniseed 24-hour continuous data and then by converting
641 the velocity ground motion (cm/s) in RMS and FFT discrete time series. The raw seismic waveforms
642 are however downloadable from the EIDA-Italia webservice (<https://eida.ingv.it/it/>).

643 For the first time, at least in Italy, high frequency and continuous multiparametric data are
644 dynamically updated daily and published soon after for end users. Data can be used for different
645 purposes, ranging from i) information regarding environmental and meteorological temporal trends
646 with respect the global climate change problematic; ii) details on local aquifer features and seismicity;

647 iii) recommendations for the civil protection; iv) multiparametric geophysical, environmental and
648 geochemical data for research studies. In particular, all seismic stations included in MUDA-db with
649 code ZO (PDnet, <https://eida.ingv.it/it/networks/network/ZO>) contribute with the national seismic
650 monitoring by sharing a continuous data stream in real time to the INGV National Seismic Network
651 (<https://eida.ingv.it/it/networks/network/IV>). In addition, the dense ZO network installed around Lake
652 Garda contribute significantly to improving the minimum magnitude threshold detection of the area
653 as reported in Ferrari et al. (2024).

654 Seismic data, together with all geological, morphological and geophysical information
655 collected at each site included in MUDA, can moreover be used to investigate the site response in
656 terms of seismic amplification, in particular for sites installed in the central part of the Po Plain, a
657 deep basin characterized by a significant thickness of incoherent alluvial deposits. Seismic events
658 recorded at each station can also be used for local investigations into the micro seismicity of the area,
659 seismic source recognition or to improve the available seismic velocity models at a local scale.

660 Hydrogeochemical and geochemical data will be used in the framework of a recent agreement
661 between the National Institute of Geophysics and Volcanology (INGV) and the National System for
662 Environmental Protection (SNPA, comprising the Regional Environmental Protection Agencies -
663 ARPA and ISPRA), aimed at gathering information on seismic activity and aquifer/spring status from
664 various acquisition sources, in some cases reaching a near real time monitoring through the SINAnet
665 facility (<https://www.snpambiente.it/attivita/sistema-informativo-nazionale-ambientale/>).

666 In general, the multiparametric monitoring is the basis by which to understand and identify
667 possible seismic precursors, an objective not yet achieved in earthquake studies. In particular, the
668 short-term earthquake forecasting, remains elusive and largely unattained. An effective solution for
669 such a major issue might be found, in the future, in systematic high frequency and continuous
670 measurements with multiparametric networks operating over the long term. Owing to the influx from
671 deep crustal fluids in active tectonic areas, groundwater monitoring may especially be considered a

672 fundamental tool for investigating pre-seismic signals of rocks undergoing accelerated strain (e.g.
673 King, 1986; Skelton, A. et al. 2014, Barberio et al., 2017).

674

675 **8 Data Availability**

676

677 Data and metadata presented and described in this manuscript can be accessed
678 under <https://doi.org/10.13127/muda> (Massa et al., 2023).

679

680 **9 Code Availability**

681

682 All the procedures to acquire and process data coming from multiparametric remote stations
683 have been specifically developed for the MUDA project in Bash scripting language, Python and PHP
684 language, using, when necessary, proprietary API taken from the manufacturers of the installed
685 remote instrumentation, as detailed in the text. Seismic data are acquired and archived through a
686 Seiscomp4 (<https://www.seiscomp.de/doc/apps/seedlink.html>) client, thereby improving the
687 SeedLink real time data acquisition protocol. Some processing steps on the seismic data are
688 undertaken using the Seismic Analysis Code (SAC,
689 <https://ds.iris.edu/ds/nodes/dmc/software/downloads/sac/>), a software designed for both real time and
690 off-line seismological analyses of time series data. The MUDA database is developed with MySQL
691 open source software. The MUDA web portal is developed in PHP and HTML5 languages, and all
692 data are published under the Creative Commons License CC BY 4.0 licence.

693

694

695

696

697

698 **Team list**

699

700 MUDA working group is at present composed by the main authors and:

701 Marino Domenico Barberio ⁽⁴⁾, Gianfranco Tamburello ⁽⁵⁾, Gioia Capelli Ghioldi ⁽⁵⁾, Santi Mirena ⁽¹⁾,

702 Ezio D'Alema ⁽¹⁾, Anna Figlioli ⁽¹⁾, Pellegrino Moretti ⁽¹⁾, Claudio Ventura Bordenca ⁽¹⁾, Fabio

703 Varchetta ⁽¹⁾, Antonio Piersanti ⁽⁴⁾, Valentina Cannelli ⁽⁴⁾, Gianfranco Galli G. ⁽⁴⁾, Rodolfo Puglia ⁽¹⁾.

704

705 ⁽¹⁾ National Institute of Geophysics and Volcanology (INGV), Milano department, Italy

706 ⁽⁴⁾ National Institute of Geophysics and Volcanology (INGV), Roma I department, Roma, Italy

707 ⁽⁵⁾ National Institute of Geophysics and Volcanology (INGV), Bologna department, Italy

708

709 **Author contributions**

710

711 This study started from an original idea by MM and ALR. MM, ALR, EF and SL contributed

712 to all phases of site installations, data acquisition, processing and archiving. DS developed MySQL-

713 Db and the associated web page, as well as the procedures to upload data into MUDA-db. SL and EF

714 contributed to organising the technical data sheet related to each multiparametric site now available

715 at each single station web page. MM developed the procedures for multiparametric data pre-

716 processing and seismic data post processing. All authors participated in the preparation of the

717 manuscript draft and in the phases of revision.

718

719 **Competing Interests: The authors declare no competing interests.**

720

721

722

723

724 **Acknowledgements**

725

726 We would like to thank all those who contributed to the site search phase and the installation
727 of the PDnet network. In particular: Prof. Tullia Bonomi (Milano Bicocca University), Engr. Michela
728 Biasibetti and Engr. Bruno Pannuzzo (Acque Bresciane company), Engr. Massimo Carmagnani and
729 Engr. Ignazio Leone (Acque Veronesi company), Engr. Giovanni Lepore and Fabrizio Brunello
730 (Azienda Gardesana Servizi company), Engr. Paolo Pizzaia (Alto Trevigiano Servizi company), Arch.
731 Luca Bertanza (municipality of Tremosine Garda, BS), Arch. Umberto Minuta (municipality of
732 Dolcè, VR), Geom. Elena Beraldini (municipality of Negrar, VR), Dr. Marzia Conventi (municipality
733 of Fiorano Modenese, MO - Dir. Riserva Salse di Nirano), Mr. Salviani (Norcia), Bagni Triponzo
734 Terme S.p.A. (municipality of Cerreto di Spoleto), Dr. Luca Martelli and Dr. Paolo Severi (Emilia
735 Romagna Region). Particular thanks go to OGS (National Institute of Oceanography and Applied
736 geophysics, <https://www.ogs.it/en>) and University of Ferrara (Department of Physics and Earth
737 Science, <http://fst.unife.it/en>) for sharing data recorded at the TOPPO site in the framework of the
738 ECCSEL-ERIC (European Research Infrastructure for CO₂ Capture, Utilisation, Transport and
739 Storage (CCUS), <https://www.eccsel.org/>) consortium.

740 The production of the seismic data published in the MUDA database involves many INGV colleagues
741 covering different tasks in the data production chain, from the correct operation of the seismic stations
742 to data acquisition, data processing, archiving and subsequent distribution. We would like to thank all
743 the colleagues of the INGV sections and offices who contribute daily to the management of the
744 National Seismic Network (RSN, <https://eida.ingv.it/it/networks/network/IV>), as well as providing
745 access to the data they produce. Finally, we thank the ESSD topic Editor, the reviewers, Dr. Simona
746 Petrosino, Dr. Galina N. Kopylova and Dr. Polina Lemenkova and the ESSD editorial team.

747

748

749

750 **References**

751

752 Aiuppa, A., Federico, C., Giudice, G., Gurrieri, S. Chemical mapping of a fumarolic field: La Fossa
753 Crater, Vulcano Island (Aeolian Islands, Italy). *Geophys. Res. Lett.* 32 (13), 1-4 (2005).

754

755 Allard, P., Burton, M., Murè F., Spectroscopic evidence for a lava fountain driven by previously
756 accumulated magmatic gas. *Nature* 433, 407-410, doi:10.1038/nature03246 (2005).

757

758 Alley, W.M., Healy, R.W., LaBaugh, J.W., Reilly, T.E., Flow and storage in groundwater systems.
759 *Science* 296 (5575), 1985-90, doi: 10.1126/science.1067123 (2002).

760

761 Barberio, M.D., Barbieri, M., Billi, A., Doglioni, C., Petitta, M., Hydrogeochemical changes before
762 and during the 2016 Amatrice Norcia seismic sequence (central Italy). *Sci. Rep. UK* 7:11735, 1-12.
763 doi:10.1038/s41598-017-11990-8 (2017).

764

765 Battaglia, M., Murray, M.H., Serpelloni, E., Bürgmann, R., The Adriatic region: an independent
766 microplate within the Africa-Eurasia collision zone. *Geophys. Res. Lett.* 31, L09605,
767 doi:10.1029/2004GL019723 (2004).

768

769 Bigi, G., Costantino, D., Parotto, M., Sartori, R., Scandone, P., Structural Model of Italy. Firenze,
770 Società Elaborazioni Cartografiche (S.EL.CA.). Consiglio Nazionale Delle Ricerche Progetto
771 Finalizzato Geodinamica, Scala 1:500.000, 9 Fogli (1990).

772

773 Bonini, M., Elliptical mud volcano caldera as stress indicator in an active compressional setting
774 (Nirano, Pede-Appennine margin, northern Italy). *Geology* 36, 131-134, doi:10.1130/G24158A.1
775 (2008).

776

777 Bormann, P., (Editor) New manual of seismological observatory practice (NMSOP-2), IASPEI, GFZ
778 German Research Centre for Geosciences, Potsdam, <https://gfzpublic.gfz-potsdam.de/> (see data and
779 resources), doi:10.2312/GFZ.NMSOP-2 (2012).

780

781 Bräuer, K., Kämpf, H., Strauch, G., Weise, S.M., Isotopic evidence ($^3\text{He}/^4\text{He}$, $^{13}\text{C}_{\text{CO}_2}$) of fluid-
782 triggered intraplate seismicity. *J. Geophys. Res.* 108(B2), 1-11, doi:10.1029/2002JB002077 (2003).

783

784 Brozzetti, F., Lavecchia, G., Seismicity and related extensional stress field: the case of the Norcia
785 Seismic Zone (Central Italy). *Annales Tectonicae* 8 (1), 36-57 (1994).

786

787 Bucci, A., Lasagna, M., De Luca, D.A., Acquavotta, F., Barbero, D., Fratianni, S., Time series analysis
788 of underground temperature and evaluation of thermal properties in a test site of the Po plain (NW
789 Italy). *Environ. Earth Sci.* 79,185, doi:10.1007/s12665-020-08920-9 (2020).

790

791 Burton, M.R., Caltabiano, T., Murè, F., Salerno, G.G., Randazzo, D., SO₂ flux from Stromboli during
792 the 2007 eruption: results from the FLAME network and traverse measurements. *J. Volcanol.*
793 *Geotherm. Res.* doi:10.1016/j.jvolgeores.2008.11.025 (2009).

794

795 Burrato, P., Vannoli, P., Fracassi, U., Basili, R., Valensise, G., Is blind faulting truly invisible?
796 Tectonic-controlled drainage evolution in the epicentral area of the May 2012, Emilia-Romagna
797 earthquake sequence (northern Italy). *Annals of Geophysics* 55, 4, 525-531 (2012).

798

799 Buttitta, D., Caracausi, A., Chiaraluce, L., Favara, R., Morticelli, M.G., Sulli, A., Continental
800 degassing of helium in an active tectonic setting (northern Italy): the role of seismicity. *Scientific*
801 *Reports* 10, Article number:162 (2020).

802

803 Cannelli, V., Piersanti, A., Galli, G., Melini, D., Italian Radon mOnitoring Network (IRON): A
804 permanent network for near real-time monitoring of soil radon emission in Italy. *Annals of geophysics*
805 4/61, 10.4401/ag-7604 (2018).

806

807 Carapezza, M.L, Inguaggiato, S., Brusca, L., Longo, M., Geochemical precursors of Stromboli 2002–
808 2003 eruptive events. *Geophys Res Lett* 31(7):10.1029/2004GL019614 (2004).

809

810 Castaldini, D., Valdati, J., Ilies, D.C., Chiriac, C., Bertogna, I., Geo-tourist map of the natural reserve
811 of Salse di Nirano (Modena Apennines, Northern Italy). *Italian Journal of Quaternary Sciences* 18(1),
812 245-255 (2005).

813

814 Cicerone, R.D., Ebel, J.E., Britton, J., A systematic compilation of earthquake precursors.
815 *Tectonophysics* 476, 371-396, doi:10.1016/j.tecto.2009.06.008 (2009).

816

817 Chiarabba, C., Piccinini, D., De Gori, P., Velocity and attenuation tomography of the Umbria Marche
818 1997 fault system: Evidence of a fluid-governed seismic sequence. *Tectonophysics* 476, 73-84,
819 doi:10.1016/j.tecto.2009.04.004 (2009).

820

821 Chiaraluce, L., Collettini, C., Cattaneo, M., Monachesi, G., The shallow boreholes at The
822 AltotiBerina near fault Observatory (TABOO; northern Apennines of Italy), Volume 17, *Scientific*
823 *Drilling*, 17, 31-35, <https://doi.org/10.5194/sd-17-31-2014> (2014).

824

825 Chiaraluce, L., Di Stefano, R., Tinti, E., Scognamiglio, L., Michele, M., Casarotti, E., Cattaneo, M.,
826 De Gori, P., Chiarabba, C., Monachesi, G., Lombardi, A., Valoroso, L., Latorre, D., Marzorati, S.

827 The 2016 Central Italy Seismic Sequence: A First Look at the Mainshocks, Aftershocks, and Source
828 Models. *Seismological Research Letters* 88 (3), 757–771 (2017).
829

830 Chiodini, G., Cioni, R., Guidi, M., Raco, B., Marini, L., Soil CO₂ flux measurements in volcanic and
831 geothermal areas. *Appl. Geochem.* 13, 543-552 (1998).
832

833 Chiodini, G., Cardellini, C., Di Luccio, F., Selva, J., Frondini, F., Caliro, S., Rosiello, A., Beddini, G.,
834 Ventura, G., Correlation between tectonic CO₂ Earth degassing and seismicity is revealed by a 10-
835 year record in the Apennines, Italy. *Sci. Adv.* 6:eabc2938, 1-7, doi:10.1126/sciadv.abc2938 (2020).
836

837 Commerci, V., Doglioni, C., Italiano, F., Baiocco, F., Barberio, M.D., Caracausi, A., Cuiuli, E., Guerra,
838 M., Infantino, V., Insolubile, M., Marcaccio, M., Martinelli, G., Menichetti, S., Onorati, G., Petitta,
839 M., Palumbo, V., Peleggi, M., Richieri, F., Scaramella, A., Scotti, E., Testa, M., Towards a national
840 hydrogeochemical monitoring system: a further tool to investigate geological hazards. *Misc. INGV*
841 49, 1-338 (2019).
842

843 D'Alessandro, A., Scudero, S., Siino, M., Alessandro, G., Mineo, R., Long-term monitoring and
844 characterization of soil radon emission in a seismically active area. *Geochem. Geophys. Geosy.*
845 21:e2020GC009061, doi:10.1029/2020GC009061 (2020).
846

847 D'Agostino, N., Avallone, A., Cheloni, D., D'Anastasio, E., S Mantenuto, Selvaggi, G., Active
848 tectonics of the Adriatic region from GPS and earthquake slip vectors. *Jour. Geophys. Res.* 113 (B12),
849 B12413 (2008).
850

851 Danecek, P., Pintore, S., Mazza, S., Mandiello, A., Fares, M., Carluccio, I., ... & Michelini, A., The
852 Italian node of the European integrated data archive. *Seismological Society of America*, 92(3), 1726-
853 1737, doi:<https://doi.org/10.1785/0220200409> (2021).

854

855 Danesi, S., Pondrelli, S., Salimbeni, S., Cavaliere, A., Serpelloni, E., Danacek P., Lovati, S., Massa,
856 M., Active deformation and seismicity in the Southern Alps (Italy): The Montello hill as a case study.
857 *Tectonophysics* 653, 95-108, doi:[10.1016/j.tecto.2015.03.028](https://doi.org/10.1016/j.tecto.2015.03.028) (2015).

858

859 De Gregorio, S., Gurrieri, S., Valenza, M., A PTFE membrane for the in situ extraction of dissolved
860 gases in natural waters: Theory and applications. *Geochem. Geophys. Geosyst.*, 6, Q09005,
861 doi:[10.1029/2005GC000947](https://doi.org/10.1029/2005GC000947) (2005).

862

863 De Gregorio, S., Federico, C., Cappuzzo, S., Favara, R., Giudice, G., Gurrieri, S., Boschi, E., Stress-
864 induced temperature variations in groundwater of the Monferrato area (north-western Italy).
865 *Geofluids* 12, 142-149, doi:[10.1111/j.1468-8123.2011.00348.x](https://doi.org/10.1111/j.1468-8123.2011.00348.x) (2012).

866

867 De Luca, G., Di Carlo, G., Tallini, M., A record of changes in the Gran Sasso groundwater before,
868 during and after the 2016 Amatrice earthquake, central Italy. *Sci. Rep. UK* 8:15982, 1-16,
869 doi:[10.1038/s41598-018-34444-1](https://doi.org/10.1038/s41598-018-34444-1) (2018).

870

871 De Matteis, R., Convertito, V., Napolitano, F., Amoroso, O., Terakawa, T., Capuano, P., Pore fluid
872 pressure imaging of the Mt. Pollino region (southern Italy) from earthquake focal mechanisms.
873 *Geophys. Res. Lett.* 48:e 2021GL094552, doi:[10.1029/2021GL094552](https://doi.org/10.1029/2021GL094552) (2021).

874

875 Di Luccio, F., Ventura, G., Di Giovambattista, R., Piscini, A., Cinti, F.R., Normal faults and thrusts
876 reactivated by deep fluids: The 6 April 2009 M_w 6.3 L'Aquila earthquake, central Italy. *J. Geophys.*
877 *Res.* 115, 1-15, doi:10.1029/2009JB007190 (2010).

878

879 DISS Working Group Database of Individual Seismogenic Sources (DISS), Version 3.3.0: A
880 compilation of potential sources for earthquakes larger than M 5.5 in Italy and surrounding areas.
881 Istituto Nazionale di Geofisica e Vulcanologia (INGV) <https://doi.org/10.13127/diss3.3.0> (2021).

882

883 Egidio, E., Mancini, S., De Luca, D.A., Lasagna, M., The Impact of Climate Change on Groundwater
884 Temperature of the Piedmont Po Plain (NW Italy). *Water* 14:2797, doi:10.3390/w14182797 (2022).

885

886 Ferrari E., Massa M., Rizzo A.L., Lovati S., Di Michele F., Multiparametric stations for real-time
887 monitoring and long-term assessment of natural hazards. *Front. Earth Sci., Sec. Geohazards and*
888 *Georisks*, Volume 12, <https://doi.org/10.3389/feart.2024.1412900> (2024).

889

890 The Italian multiparametric network for detection and monitoring of earthquake-related crustal fluids
891 alterations. EGU meeting, Wien, session SM3.4, 14-19 April (2024).

892

893 Gabrielli, S., Akinci, A., Ventura, G., Napolitano, F., Del Pezzo, E., De Siena, L., Fast changes in
894 seismic attenuation of the upper crust due to fracturing and fluid migration: the 2016–2017 Central
895 Italy seismic sequence. *Front. Earth Sci.* 10:909698, doi: 10.3389/feart.2022.909698 (2022).

896

897 Gabrielli, S., Akinci, A., De Siena, L., Del Pezzo, E., Buttinelli, M., Maesano, F.E., Maffucci, R.,
898 Scattering attenuation images of the control of thrusts and fluid overpressure on the 2016–2017
899 Central Italy seismic sequence. *Geophys. Res. Lett.* 50:e2023GL103132,
900 doi:10.1029/2023GL103132 (2023).

901

902 Galadini, F., Galli, P., The Holocene paleoearthquakes on the 1915 Avezzano earthquake faults
903 (central Italy): implications for active tectonics in the central Apennines. *Tectonophysics* 308, 1-2,
904 143-170 (1999).

905

906 Galadini, F., Messina, P., Plio-Quaternary changes of the normal fault architecture in the Central
907 Apennines (Italy). *Geodinamica Acta*, 321-344, <https://doi.org/10.1080/09853111.2001.10510727>
908 (2001).

909

910 Galli, P., Galderisi, A., Ilardo, I., Piscitelli, S., Scionti, V., Bellanova, J., & Calzoni, F., Holocene
911 paleoseismology of the Norcia fault system (central Italy). *Tectonophysics* 745, 154-169,
912 <https://doi.org/10.1016/j.tecto.2018.08.008> (2018).

913

914 Galli, P., Galderisi, A., Peronace, E., Giaccio, B., Hajdas, I., Messina, P., Pileggi, D., Polpetta, F. The
915 Awakening of the Dormant Mount Vettore Fault (2016 Central Italy Earthquake, Mw 6.6):
916 Paleoseismic Clues on Its Millennial Silences. *Tectonics* <https://doi.org/10.1029/2018TC005326>
917 (2019).

918

919 Gerten, D., Hoff, H., Rockström, J., Jägermeyr, J., Kummu, M., Pastor, A.V., Towards a revised
920 planetary boundary for consumptive freshwater use: role of environmental flow requirements.
921 *Environmental Sustainability* 5, issue 6, 551-558 (2013).

922

923 Giambastiani, B.M.S., Chiapponi, E., Polo, F., Nespoli, M., Piombo, A., Antonellini, M., Structural
924 control on carbon emissions at the Nirano mud volcanoes – Italy. *Marine and Petroleum Geology*
925 163, 106771 (2024).

926

927 Goldstein, P., Dodge, D., Firpo, M., Minner, L., SAC2000: Signal processing and analysis tools for
928 seismologists and engineers, Invited contribution to “The IASPEI International Handbook of
929 Earthquake and Engineering Seismology”, Edited by WHK Lee, H. Kanamori, P.C. Jennings, and C.
930 Kisslinger, Academic Press, London (2003).

931

932 Gori, F., Barberio, M.D., Hydrogeochemical changes before and during the 2019 Benevento seismic
933 swarm in central-southern Italy. *J. Hydrol.* 604:127250, 1-10, doi:10.1016/j.jhydrol.2021.127250
934 (2022).

935

936 Guillaumot, L., Longuevergne, L., Marçais, J., Lavenant, N., Bour, O., Frequency domain water table
937 fluctuations reveal impacts of intense rainfall and vadose zone thickness on groundwater recharge.
938 *Hydrology and Earth System Sciences* 26, issue 22, HESS, 26, 5697–5720,
939 <https://doi.org/10.5194/hess-26-5697-2022> (2022).

940

941 Hubbert, M.K., Rubey, W.W., Role of fluid pressure in mechanics of overthrust faulting: mechanics
942 of fluid-filled porous solids and its application to overthrust faulting. *Geol. Soc. Am. Bull.* 70(2), 115-
943 166, doi:10.1130/0016-7606(1959)70[115:ROFPIM] 2.0.CO;2 (1959).

944

945 Improta, L. and co-Authors Multi-segment rupture of the 2016 Amatrice-Visso-Norcia seismic
946 sequence (central Italy) constrained by the first high-quality catalog of Early Aftershocks. *Scientific*
947 *Reports*, 9, 6921 (2019).

948

949 Inguaggiato, S., Vita, F., Rouwet, D., Bobrowski, N., Morici, S., Sollami, A., Geochemical evidence
950 of the renewal of volcanic activity inferred from CO₂ soil and SO₂ plume fluxes: the 2007 Stromboli
951 eruption (Italy). *Bulletin of Volcanology* <http://dx.doi.org/10.1007/s00445-010-0442-z> (2011a).

952

953 Inguaggiato, S., Calderone, L., Inguaggiato, C., Morici, S. and Vita, F., Dissolved CO₂ in natural
954 waters: development of an automated monitoring system and first application to Stromboli volcano
955 (Italy). *Annals of Geophysics* 54(2), doi: 10.4401/ag-5180 (2011b).
956

957 Italiano, F., Martinelli, G., Rizzo, A., Geochemical evidence of seismogenic-induced anomalies in the
958 dissolved gases of thermal waters: A case study of Umbria (Central Apennines, Italy) both during and
959 after the 1997-1998 seismic swarm. *Geochem. Geophys. Geosy.* 5(11), 1-11,
960 doi:10.1029/2004GC000720 (2004).
961

962 Italiano, F., Martinelli, G., Nuccio, P.M., Anomalies of mantle-derived helium during the 1997-1998
963 seismic swarm of Umbria-Marche, Italy. *Geophys. Res. Lett.* 28(5), 839-842,
964 doi:10.1029/2000GL012059 (2001).
965

966 Keranen, K.M., Weingarten, M., Induced seismicity. *Annu. Rev. Earth Pl. Sc.* 46, 149-174.
967 doi:10.1146/annurev-earth-082517-010054 (2018).
968

969 King, C.Y., Gas geochemistry applied to earthquake prediction: An overview, *Journal of Geophysical*
970 *Research.* <https://doi.org/10.1029/JB091iB12p12269> (1986).
971

972 Lai, C.G., Poggi, V., Famà, A., Zuccolo, E., Bozzoni, F., Meisina, C., Bonì, R., Martelli, L., Massa,
973 M., Mascandola, C., Petronio, L., Affatato, A., Baradello, L., Castaldini, D., Cosentini, R.M., An
974 inter-disciplinary and multi-scale approach to assess the spatial variability of ground motion for
975 seismic microzonation: the case study of Cavezzo municipality in Northern Italy, *Eng. Geol.* 274,
976 105722, <https://doi.org/10.1016/j.enggeo.2020.105722> (2020).
977

978 Lee, H.A., Hamm, S.Y., Woo, N.C., Pilot-scale groundwater monitoring network for earthquake
979 surveillance and forecasting research in Korea. *Water* 13:2448, 1-19, doi:10.3390/w13172448
980 (2021).

981

982 Locati, M., Camassi, R., Rovida, A., Ercolani, E., Bernardini, F., Castelli, V., Caracciolo, C.H.,
983 Tertulliani, A., Rossi, A., Azzaro, R., D'Amico, S., Conte, S., Rocchetti, E., Antonucci, A., Database
984 Macrosismico Italiano (DBMI15), versione 4.0. Istituto Nazionale di Geofisica e Vulcanologia
985 (INGV), <https://doi.org/10.13127/dbmi/dbmi15.4> (2022).

986

987 Luzi, L., Pacor, F., Ameri, G., Puglia, R., Burrato, P., Massa, M., Augliera, P., Castro, R.,
988 Franceschina, G., Lovati, S. Overview on the strong motion data recorded during the May-June 2012
989 Emilia seismic sequence. *Seism. Res. Lett.*, 84, 4, 629-644 (2013).

990

991 Luzi, L., Puglia, R., Russo, E., D'Amico, M., Felicetta, C., Pacor, F., Lanzano, G., Çeken, U.,
992 Clinton, J., Costa, G., et al. The European strong-motion database: a platform to access accelerometric
993 data. *Seismol. Res. Lett.* 87, 4, doi: 10.1785/0220150278 (2016).

994

995 Malagnini, L., Pio Lucente, F., De Gori, P., Akinci, A., Munafo', I., Control of pore fluid pressure
996 diffusion on fault failure mode: Insights from the 2009 L'Aquila seismic sequence. *J. Geophys. Res-*
997 *Sol. Ea.* 117, 1-15, doi:10.1029/2011JB008911 (2012).

998

999 Mancini, S., Egidio, E., De Luca, D.A., Lasagna, M., Application and comparison of different
1000 statistical methods for the analysis of groundwater levels over time: Response to rainfall and resource
1001 evolution in the Piedmont Plain (NW Italy). *Science of the total Environment* 846, 157479 (2022).

1002

1003 Marchetti, A. and co-Authors The Italian Seismic Bulletin: strategies, revised pickings and locations
1004 of the central Italy seismic sequence. *Annals of Geophysics FAST TRACK* 5/59, 10.4401/ag-7169
1005 (2016).

1006

1007 Margheriti, L. and co-Authors Seismic Surveillance and Earthquake Monitoring in Italy.
1008 *Seismological Research Letters* 92 (3): 1659-1671 (2021).

1009

1010 Martinelli, G., Contributions to a history of earthquake prediction research. In *Pre-earthquake*
1011 *processes: a multidisciplinary approach to earthquake prediction studies*. Editors Ouzounov, D.,
1012 Pulinets, S., Hattori, K., Taylor, P. John Wiley & Sons (2018).

1013

1014 Martinelli, G., Ciolini, R., Facca, G., Fazio, F., Gherardi, F., Heinicke, J., Pierotti, L., Tectonic-related
1015 geochemical and hydrological anomalies in Italy during the last fifty years. *Minerals* 11:107, 1-16,
1016 doi:10.3390/min11020107 (2021).

1017

1018 Massa M., Rizzo L.A., Ferrari E., Lovati S., Scafidi D., Puglia R., Varchetta F., D'Alema E., Mirena
1019 S., Luzi L., MUDA geophysical and geochemical MULTiparametric DAtabase,
1020 <https://doi.org/10.13127/muda> (2023).

1021

1022 Massa, M., Marzorati,S., D'Alema, E., Di Giacomo, D., Augliera, P., Site Classification Assessment
1023 for Estimating Empirical Attenuation Relationships for Central-Northern Italy Earthquakes. *Journal*
1024 *Earth. Eng.* 11:6, 943-967 (2007).

1025

1026 Massa, M., Rizzo, A.L., Lorenzetti, A., Lovati, S., D'Alema, E., Puglia, R., Carannante, S., Piersanti,
1027 A., Galli, G., Cannelli, V., Luzi, L., blog INGV Terrermoti, <https://ingvterremoti.com/2021/12/10/la->

1028 rete-del-lago-di-garda-una-nuova-infrastruttura-dellingv-per-il-monitoraggio-multiparametrico/ (in
1029 Italian) (2021).

1030

1031 Massa, M., Lovati, S., Puglia, R., Brunelli, G., Lorenzetti, A., Mascandola, C., Felicetta, C., Pacor,
1032 F., Luzi, L., Seismo-Stratigraphic Model for the Urban Area of Milan (Italy) by Ambient-Vibration
1033 Monitoring and Implications for Seismic Site Effects Assessment. *Frontiers in Earth Science* doi:
1034 10.3389/feart.2022.915083 (2022b).

1035

1036 Massa, M., Scafidi, D., Mascandola, C., Lorenzetti, A., Introducing ISMDq—A Web Portal for Real-
1037 Time Quality Monitoring of Italian Strong-Motion Data. *Seismol. Res. Lett.* 93 (1), 241-256,
1038 doi:10.1785/0220210178 (2022).

1039

1040 Mastrorillo, L., Saroli, M., Viaroli, F., Banzato, F., Valigi, D., Petitta, M., Sustained post-seismic
1041 effects on groundwater flow in fractured carbonate aquifers in Central Italy. *Hydrological Processes*
1042 <https://doi.org/10.1002/hyp.13662> (2020).

1043

1044 Mazzoli, S., Santini, S., Macchiavelli, C., Ascione, A., Active tectonics of the outer northern
1045 Apennines: Adriatic vs. Po Plain seismicity and stress fields. *Journal of Geodynamics* 84, 62-76
1046 (2015).

1047

1048 McNamara, D.E., Buland, R.P., Ambient Noise Levels in the Continental United States. *Bull. Seism.*
1049 *Soc. Am.* 94, 4, 1517-1527, <https://doi.org/10.1785/012003001> (2004).

1050

1051 Menberg, K., Blum, P., Kurylyk, B.L., Bayer, P., Observed groundwater temperature response to
1052 recent climate change. *Hydrol. Earth Syst. Sci.* 18, 4453-4466, doi:10.5194/hess-18-4453-2014
1053 (2014).

1054

1055 Michelini, A., Faenza, L., Lanzano, G., Lauciani, V., Jozinović D., Puglia, R., Luzi, L., The New
1056 ShakeMap in Italy: Progress and Advances in the Last 10 Yr. *Seismological Research Letters* 91 (1),
1057 317-333 (2020).

1058

1059 Miller, S.A., Collettini, C., Chiaraluce, L., Cocco, M., Barchi, M., Kaus, B.J.P., Aftershocks driven
1060 by a high-pressure CO₂ source at depth. *Nature* 427, 724-727, doi:10.1038/nature02251 (2004).

1061

1062 Ministero delle Infrastrutture e dei Trasporti Aggiornamento delle Norme Tecniche per le
1063 Costruzioni. Part 3.2.2: Categorie di sottosuolo e condizioni topografiche (in Italian), *Gazzetta*
1064 Ufficiale n. 42 (2018).

1065

1066 Massa M., Rizzo L.A., Ferrari E., Lovati S., Scafidi D., Puglia R., Varchetta F., D'Alema E., Mirena
1067 S., Luzi L., MUDA: geophysical and geochemical MUltiparametric Database,
1068 <https://doi.org/10.13127/muda> (2023).

1069

1070 Nakamura, Y. (1989). A method for dynamic characteristics estimation of subsurface using
1071 microtremor on the ground surface, *Q. Rep. Railway Tech. Res. Inst.* 30, no. 1, 25–33.

1072

1073 Napolitano, F., De Siena, L., Gervasi, A., Guerra, I., Scarpa, R., La Rocca, M., Scattering and
1074 absorption imaging of a highly fractured fluid-filled seismogenetic volume in a region of slow
1075 deformation. *Geosci. Front.* 11, 989-998, doi:10.1016/j.gsf.2019.09.014 (2020).

1076

1077 Pacor, F., Paolucci, R., Ameri, G., Massa, M., Puglia R., Italian strong motion records in ITACA:
1078 Overview and record processing. *Bull. Earthq. Eng.* 9, 6, 1741-1759 (2011).

1079

1080 Pessina, V., Fiorini, E., A GIS procedure for fast topographic characterization of seismic recording
1081 stations. *Soil Dynam. Earthq. Eng.* 63, 248-258 (2014).
1082

1083 Pieri, M., Groppi, G., Subsurface Geological Structure of the Po Plain, Italy. Progetto Finalizzato
1084 Geodinamica/Sottoprogetto “Modello Strutturale” (Rome: Consiglio Nazionale delle Ricerche Publ.
1085 N° 414) (1981).
1086

1087 Pondrelli, S., Ekström, G., Morelli, A., Seismotectonic re-evaluation of the 1976 Friuli, Italy, seismic
1088 sequence. *Journal of Seism.*, 5, 73-83 (1999).
1089

1090 Rikitake, T., Hamada, K., Earthquake prediction. In: *Encyclopaedia of Physical Science and*
1091 *Technology*, 3rd edition, Academic Press, San Diego, CA, USA 4, 743-760 (2001).
1092

1093 Rizzo, A.L., Federico, C., Inguaggiato, S., Sollami, A., Tantillo, M., Vita, F., Bellomo, S., Longo,
1094 M., Grassa, F., Liuzzo, M., The 2014 Effusive Eruption at Stromboli Volcano (Italy): Inferences From
1095 Soil CO₂ Flux and 3He/4He Ratio in Thermal Waters. *Geoph. Res. Lett.*
1096 <http://dx.doi.org/10.1002/2014GL062955> (2015).
1097

1098 Romano, D., Sabatino, G., Magazù, S., Di Bella, M., Tripodo, A., Gattuso, A., Italiano, F.,
1099 *Environmenta Earth Sciences* 82, 273 (2023).
1100

1101 Russo, T.A., Lall, U., Depletion and response of deep groundwater to climate-induced pumping
1102 variability. *Nature Geoscience* 10, 105-108 (2017).
1103

1104 Rovida, A., Locati, M., Camassi, R., Lolli, B., Gasperini, P., The Italian Earthquake Catalogue
1105 CPTI15. *Bull. Earthq. Eng.* 18 (7), 2953-2984, doi:10. 1007/s10518-020-00818-y (2020).

1106

1107 Scognamiglio, L., Tinti, E., Michelini, A., Dreger, D.S., Cirella, A., Cocco, M., Salvatore, M.,
1108 Piatanesi, A., Fast Determination of Moment Tensors and Rupture History: What Has Been Learned
1109 from the 6 April 2009 L'Aquila Earthquake Sequence. *Seism. Res. Lett.* 81(6): 892-906 (2009).

1110

1111 Serpelloni, E., Anzidei, M., Baldi, P., Casula, G., Galvani, A., Crustal Velocity and Strain-Rate fields
1112 in Italy and Surrounding Regions: New Results From the Analysis of Permanent and Non- Permanent
1113 GPS Networks. *Geophys. J. Int.*, 161, 3, 861-880 (2005).

1114

1115 Shinohara, H., A new technique to estimate volcanic gas composition: plume measurements with a
1116 portable multi-sensor system. *J. Volcanol. Geotherm. Res.* 143, 319-333 (2005).

1117

1118 Skelton, A., and co-Authors Changes in groundwater chemistry before two consecutive earthquakes
1119 in Iceland. *Nature Geoscience* 7, 752-756 (2014).

1120

1121 Stucchi, M., Meletti, C., Montaldo, V., Crowley, H., Calvi, G.M., Boschi, E., Seismic Hazard
1122 Assessment (2003-2009) for the Italian building code. *Bull. Seism. Soc. Am.* 101, 1885-1911 (2011).

1123

1124 Taylor, C.A., Stefan, H.G., Shallow groundwater temperature response to climate change and
1125 urbanization. *J. Hydrol.* 375, 601-612, doi:10.1016/j.jhydrol.2009.07.009 (2009).

1126

1127 Ventura, G., Di Giovambattista, R., Fluid pressure, stress field and propagation style of coalescing
1128 thrusts from the analysis of the 20 May 2012 M_L 5.9 Emilia earthquake (Northern Apennines, Italy).
1129 *Terra Nova* 25, 72-78, doi: 10.1111/ter.12007 (2012).

1130

1131 Weiss, A., Topographic position and landform analysis. 21st Annual Esri International User
1132 Conference, San Diego, California, 9-13 July (2001).

1133

1134 **Figure Captions**

1135

1136 **Figure 1** - MUDA home page: <https://muda.mi.ingv.it>. Examples of interactive pop-ups are reported
1137 in map indicating the available main options concerning stations data and metadata, Italian seismic
1138 hazard (Stucchi et al., 2011), seismicity rate and both composite and single seismogenic sources
1139 (DISS database, DISS Working Group 2021). The base map is provided by ©OpenStreetMap
1140 contributors 2024. Distributed under the Open Data Commons Open Database License (ODbL) v1.0.

1141

1142 **Figure 2** - Target areas and relative multiparametric sites. Each panel indicates the multiparametric
1143 site (yellow triangles), the Italian seismic hazard map in terms of horizontal peak ground acceleration
1144 (PGA) with 10% probability of exceedance in 50 years on hard ground (Stucchi et al., 2011), the
1145 instrumental seismicity from 1985 (black circles, <https://terremoti.ingv.it>), the historical seismicity
1146 (red circles, CPTI database, Rovida et al., 2020) and the seismogenic sources (CSS-DISS database,
1147 DISS Working Group 2021). The base maps are provided by ©OpenStreetMap contributors 2024.
1148 Distributed under the Open Data Commons Open Database License (ODbL) v1.0.

1149

1150 **Figure 3** - Dynamic multiparametric data web page: <https://muda.mi.ingv.it/dat.php>. From top to
1151 bottom: hydrogeochemical data (light blue panels: water level, m; water electrical conductivity,
1152 $\mu\text{S}/\text{cm}$; water temperature, $^{\circ}\text{C}$), meteorological data (green panel: soil temperature, $^{\circ}\text{C}$; rain, mm),
1153 seismic data (light brown panels: RMS, ground motion velocity, cm/s ; FFT, $\text{cm}/\text{s}/\text{Hz}$; FFT(f),
1154 $\text{cm}/\text{s}/\text{Hz}$), CO_2 data (grey panels: soil flux, $\text{g}\cdot\text{m}^{-2}\cdot\text{d}^{-1}$; humidity, %; soil temperature, $^{\circ}\text{C}$), Radon data
1155 on air (yellow panel: Bq/m^3). All time series (*csv* format) and each single graph (*pdf*, *png* formats)
1156 are downloadable by using the menu available in the top right corner of each panel.

1157

1158 **Figure 4** - Multiparametric site web page: <https://muda.mi.ingv.it/stazione.php>. The single site web
1159 page indicates the main features of both instrumentation and installation, downloadable thematic
1160 maps such as the geological map (1:100.000, Società Geologica Italiana
1161 <http://www.isprambiente.gov.it/it/cartografia/>), the topographic map (base at 1:25.000, Istituto
1162 Geografico Militare, http://www.igmi.org/prodotti/cartografia/carte_topografiche/), log and
1163 stratigraphy concerning the available wells for water, a preliminary geophysical soil characterization
1164 in term of horizontal to vertical spectral ratio performed on ambient seismic noise and the complete
1165 time hydrogeochemical time series. Sources for base maps: Esri, DigitalGlobe, GeoEye, i-cubed,
1166 USDA FSA, USGS, AEX, Getmapping, Aerogrid, IGN, IGP, swisstopo, and the GIS User
1167 Community.

1168

1169 **Figure 5** - MUDA data base scheme and processing flow chart.

1170

1171 **Figure 6** - Single station data set for multiparametric sites having at least 6 months of data and three
1172 different types of acquisition. S: seismic data (red); Id: hydrogeochemical data (blue); M:
1173 meteorological data (green); R: Radon data (grey); C: CO₂ data (yellow). Yellow and orange stars
1174 indicate recorded earthquakes at each site with magnitude (Moment or Local) lower and higher than
1175 4, respectively.

1176

1177 **Figure 7** - Quality check of seismic data at Oppeano site (table 1).

1178 Panel *a* (top): timeseries recorded on December, 29, 2020, by IV.OPPE station
1179 (<https://terremoti.ingv.it/instruments/station/OPPE>) showing consecutive earthquakes: the first, with
1180 $M_w=6.3$, occurred in Croatia land (<https://terremoti.ingv.it/event/25870121>) 450 km East of IV.OPPE
1181 and the others with epicentres 11 km South-West of IV.OPPE with maximum $M_w=3.9$

1182 (<https://terremoti.ingv.it/event/25871441>). Earthquakes origin times (UTC) are reported in the top
1183 panel *a*).

1184 The bottom panel *a*) shows the FFT functions calculated considering 15 frequency intervals from 0.1
1185 to 20 Hz, considering 288 consecutive 5 minutes-time windows (i.e. 24 hours) selected on the vertical
1186 component of motion.

1187 Panel *b*: from top to bottom, the RMS, the ground motion velocity and the mean FFT calculated for
1188 288 consecutive time windows with duration of 5 minutes. Red, blue and green indicate the vertical,
1189 the North-South and the East-West horizontal components of motion. The black solid lines indicate
1190 the cumulative functions.

1191

1192 **Figure 8** - Example of multiparametric data recorded at Bondo site (table 1). Panel *a* shows the
1193 hydrogeochemical data recorded in the time period from October 15 to November 15, 2023: black,
1194 red and green solid lines indicate the water level (m), the electrical conductivity ($\mu\text{S}/\text{cm}$) and the
1195 water temperature ($^{\circ}\text{C}$) variations, respectively.

1196 The panel *b* shows the seismic data recorded at ZO.PDN3 station (table 2) on October, 31 and
1197 November, 1, 2023, while the panel *c* shows the polarization analysis in terms of rotated horizontal
1198 to vertical spectral ratio.

1199

1200 **Figure 9** - Radon time series (Bq/m^3 , black lines) recorded at Bondo (panel *a*) and Montelungo (panel
1201 *b*) multiparametric sites. Soil temperature ($^{\circ}\text{C}$, green lines) and rain (mm, light blue lines) are also
1202 indicated. At the top of each panel seasons are indicated (Aut=Autumn, Win=Winter, Spr=Spring,
1203 Sum=Summer).

1204

1205 **Figure 10** - Panel *a*: CO_2 flux ($\text{g}\cdot\text{m}^{-2}\cdot\text{d}^{-1}$, black line) recorded at NIRANO multiparametric site. Red
1206 and green solid lines indicate the smoothing function of CO_2 flux and the temperature ($^{\circ}\text{C}$),
1207 respectively. The orange box indicates the time window represented in the bottom panel.

1208 Panel *b*: detailed monitoring for period October 25 to November 15, 2023, where a seismic sequence,
1209 with maximum local magnitude of 3.5 (vertical yellow dashed lines) occurred in correspondence of
1210 the Nirano's Mud-Volcanoes. Dotted and dashed orange lines indicate the mean values +/- 1-standard
1211 deviation of CO₂ flux recorded during the analysed time period. Rain values (mm, light blue) and soil
1212 temperature (°C) are also indicated. Black dots indicate the CO₂ measures (g*m⁻²*d⁻¹).

1213

1214 **Figure 11** - Groundwater recharge at Volargne (panel *a*) and Fonte (panel *b*) sites (table 1) recorded
1215 on October 30, 2023. In both panels, black, red and green solid lines indicate the water level (m), the
1216 electrical conductivity (µS/cm) and the water temperature (°C) variations, respectively, while the blue
1217 solid lines indicate the cumulative rain.

1218

1219 **Table captions**

1220

1221 **Table 1** - Monitoring multiparametric sites at present include in MUDA.

1222

1223 **Table 2** - Main features of hydrogeochemical probes and seismic monitoring stations. Grey cells
1224 indicate well with thermalism (i.e. Triponzo site), while the black cells indicate the borehole seismic
1225 sensor installed 150 m depth at Oppeano site.

1226 In detail,

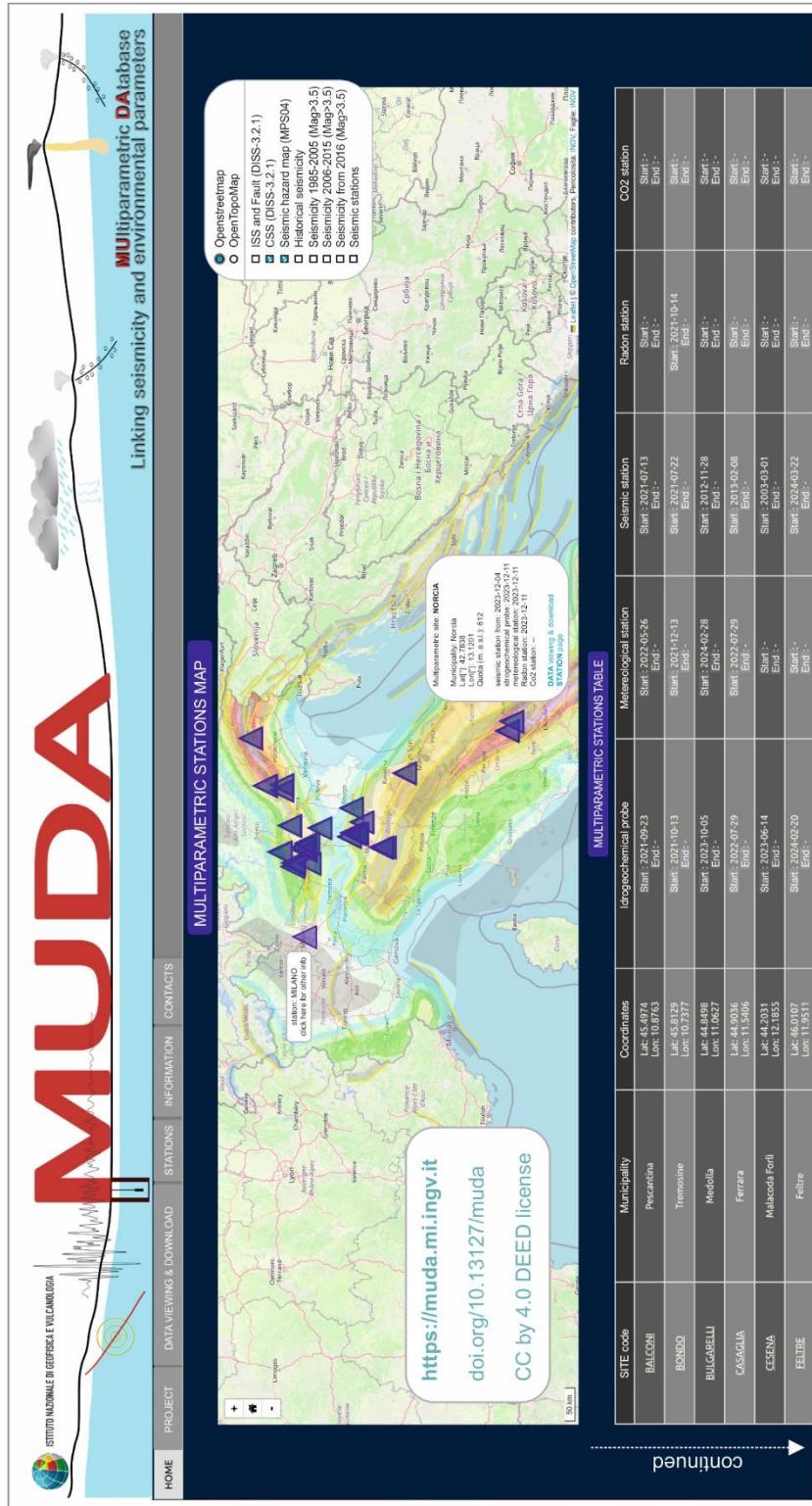
1227 water level: water depth below ground level at the time of installation;

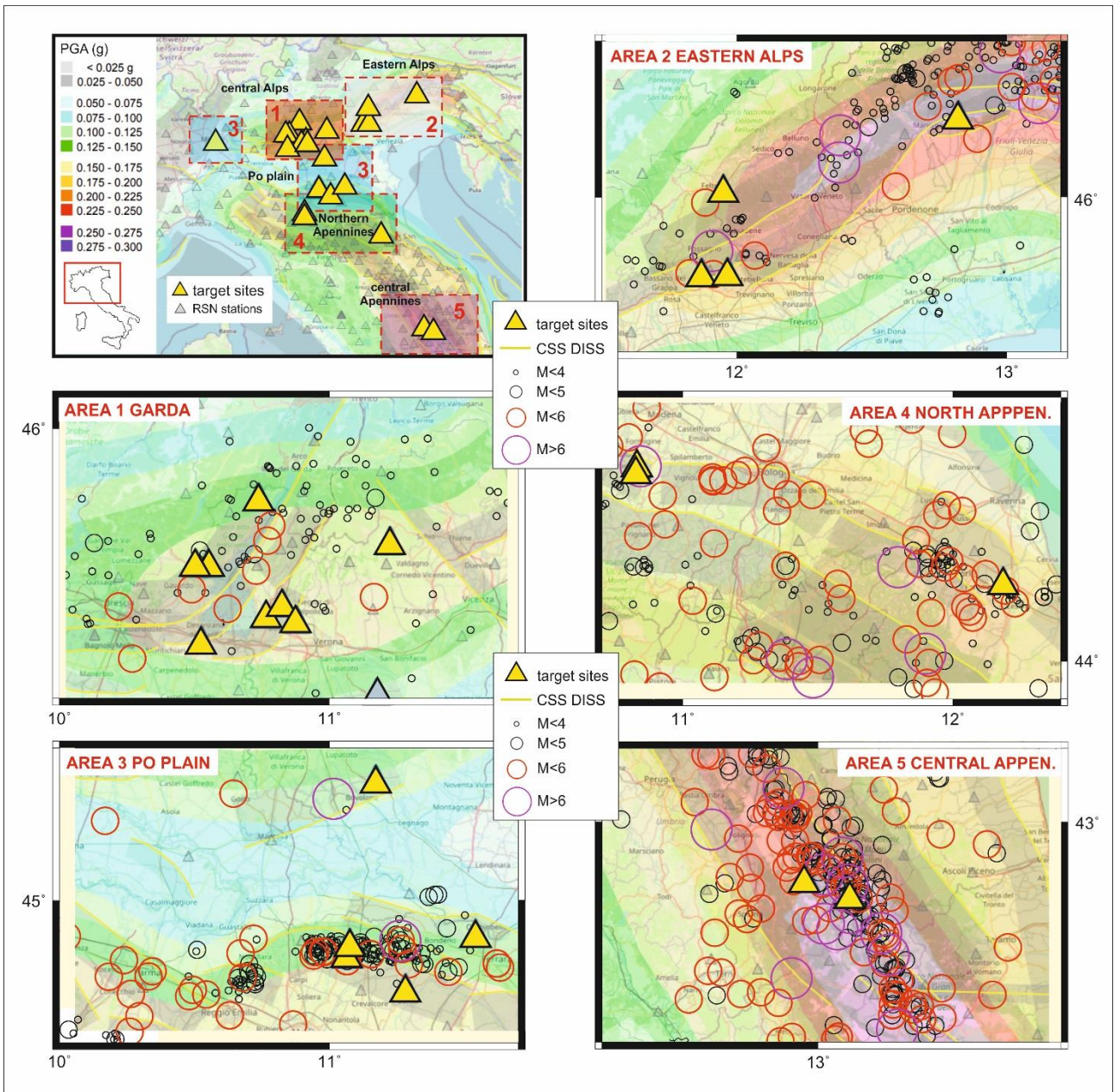
1228 water column: water column above the sensor at the time of installation;

1229 water temperature: average values of water temperature and specific electrical conductivity. It is
1230 worth noting that for some sites the averages are merely indicative as they refer to short recording
1231 intervals (see Table 1 for installation dates). Specific electrical conductivity is recalculated at 25 °C.

1232 water pump: absence (0) or presence (1) of water pump.

1233





1238

1239

1240 Figure 2

1241

1242

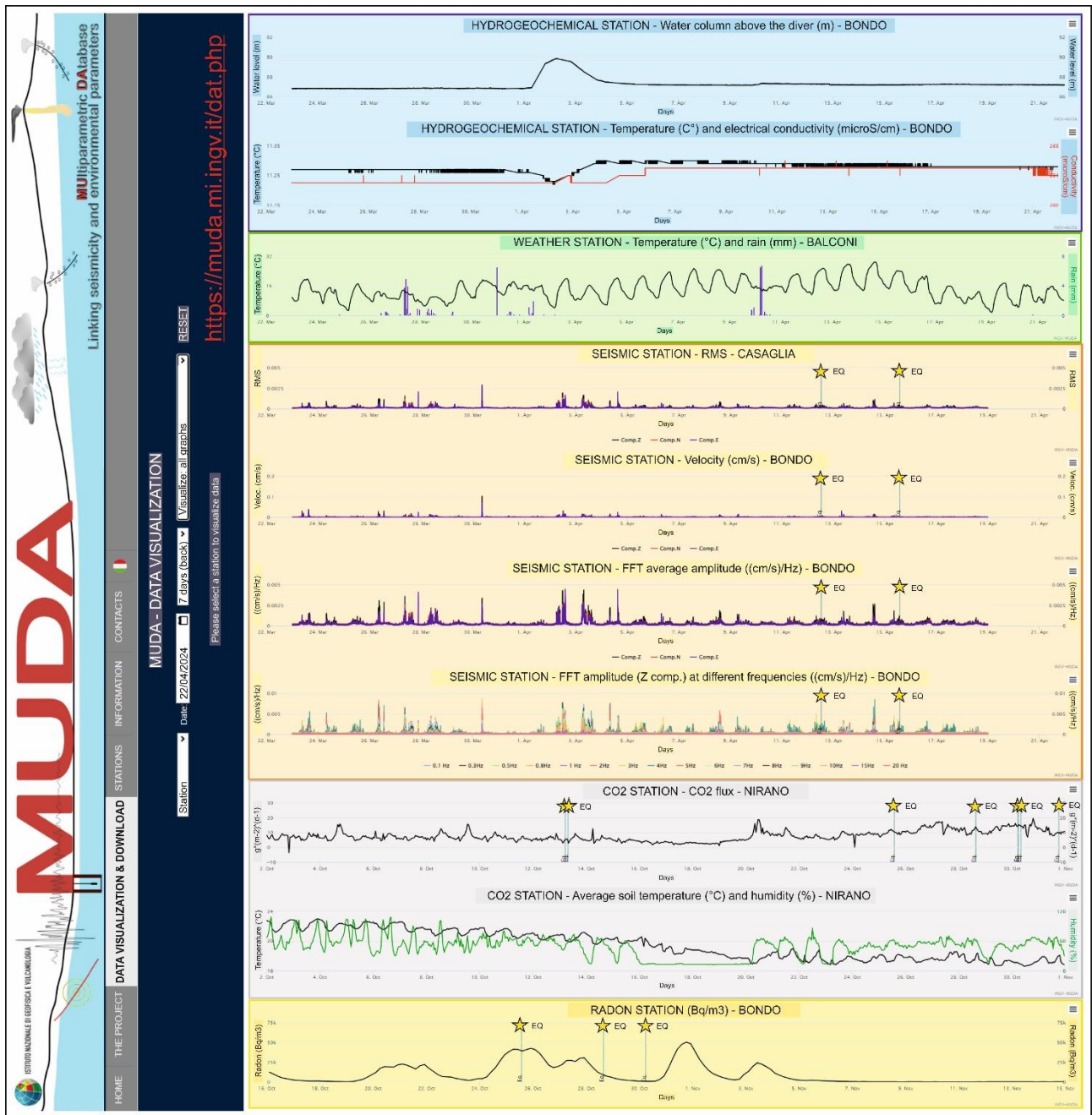
1243

1244

1245

1246

1247



1248

1249

1250 Figure 3

1251

1252

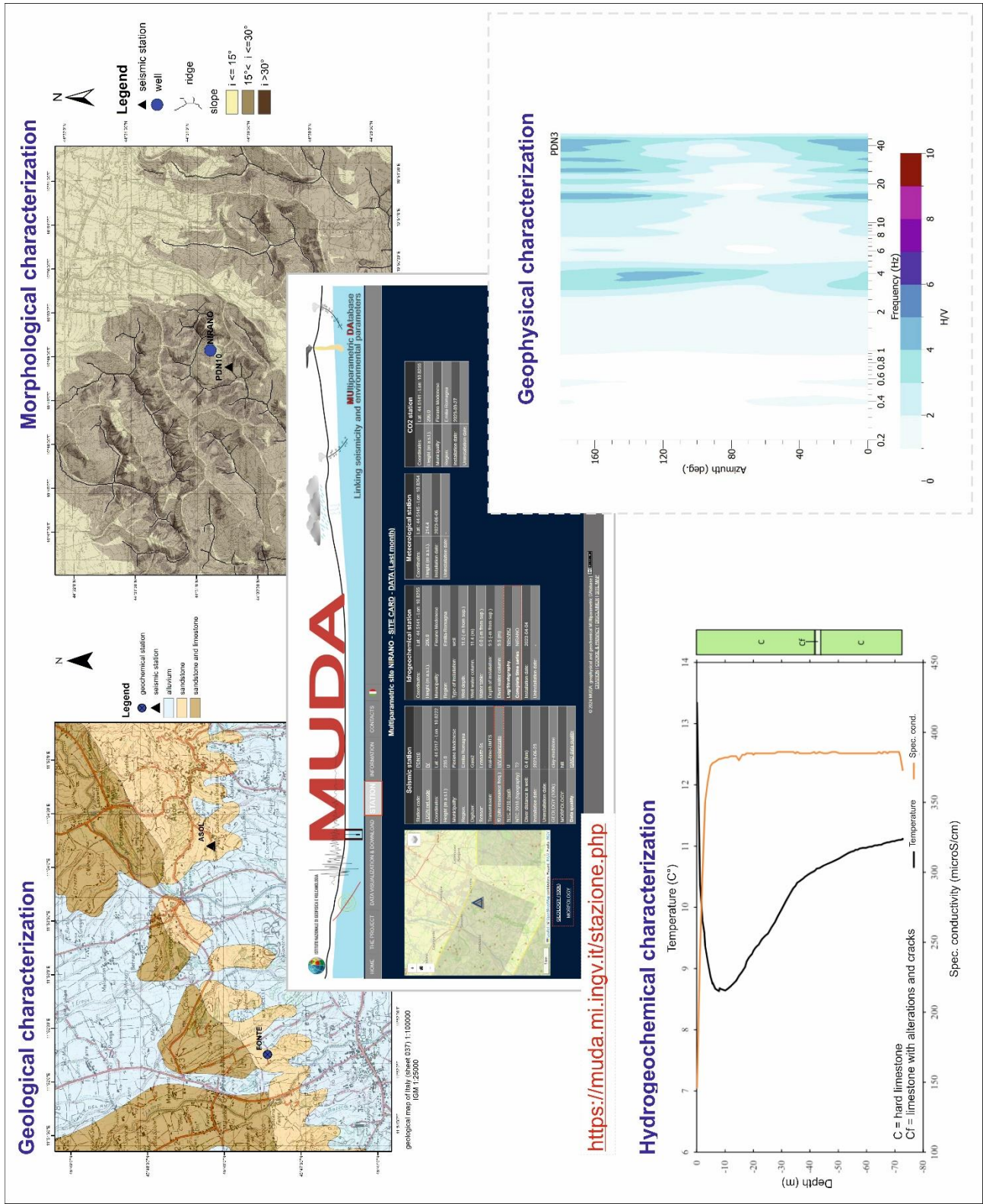
1253

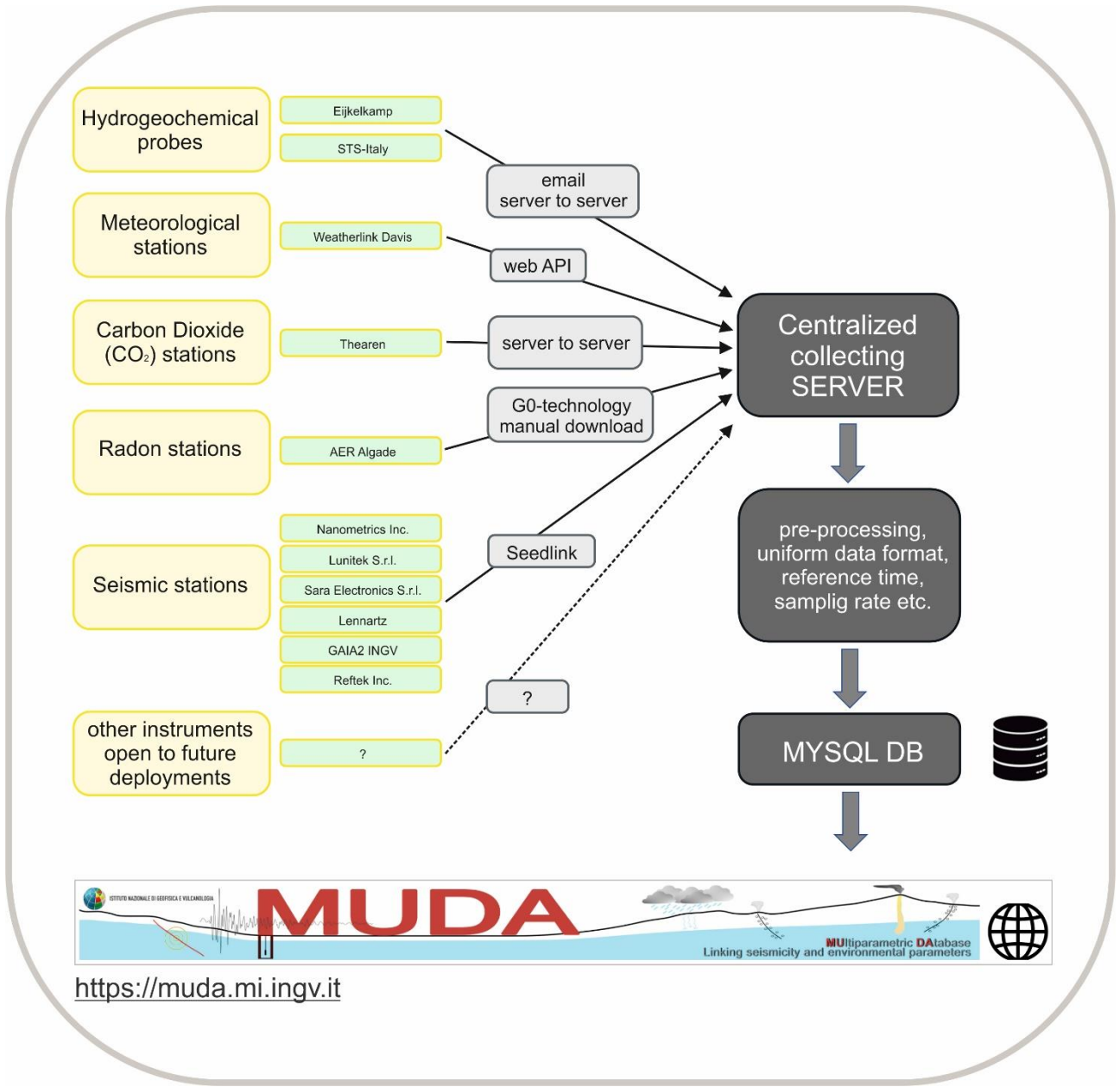
1254

1255

1256

1257
 1258
 1259
 1260
 1261





1262

1263

1264 Figure 5

1265

1266

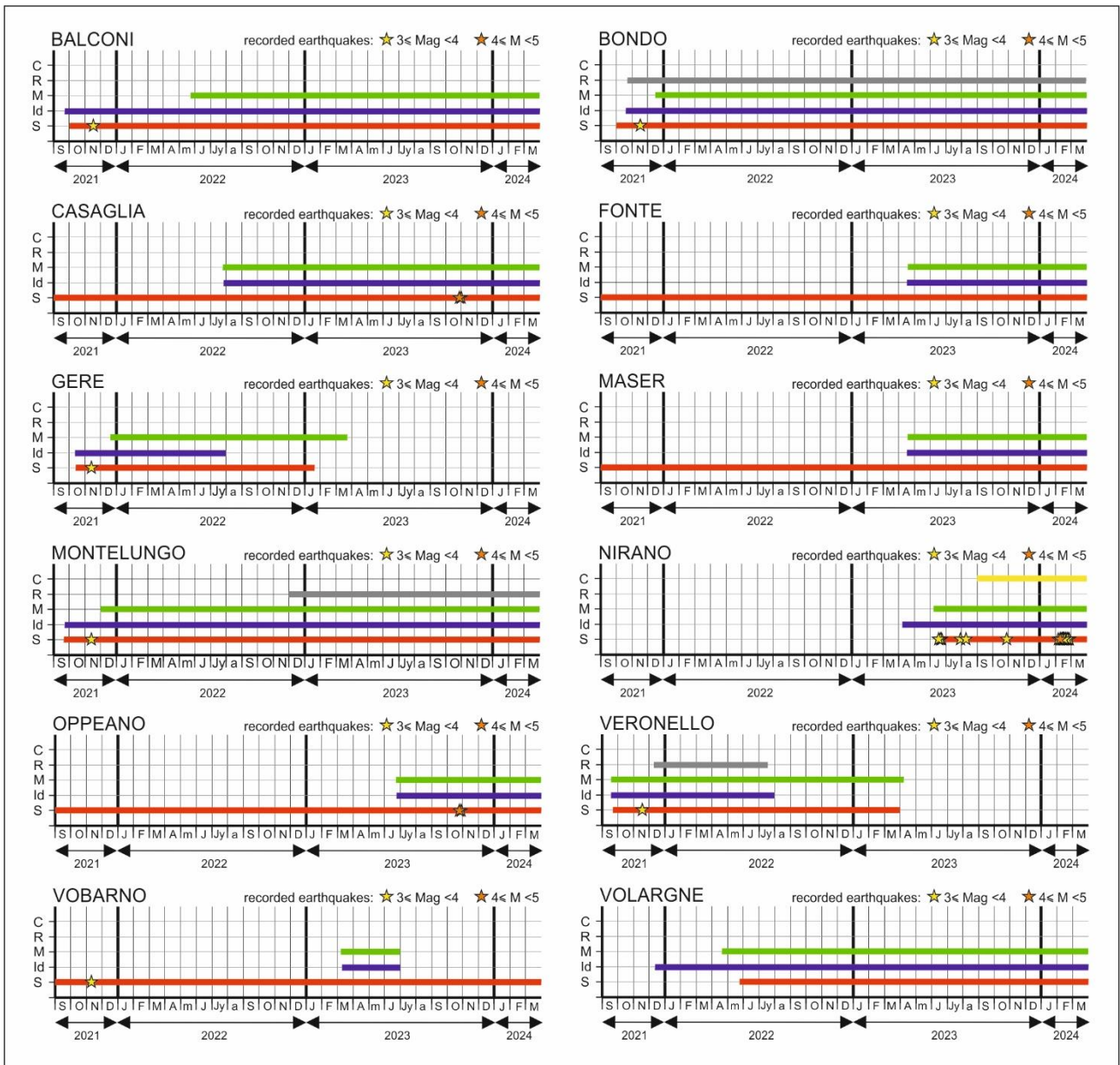
1267

1268

1269

1270

1271



1272

1273

1274 Figure 6

1275

1276

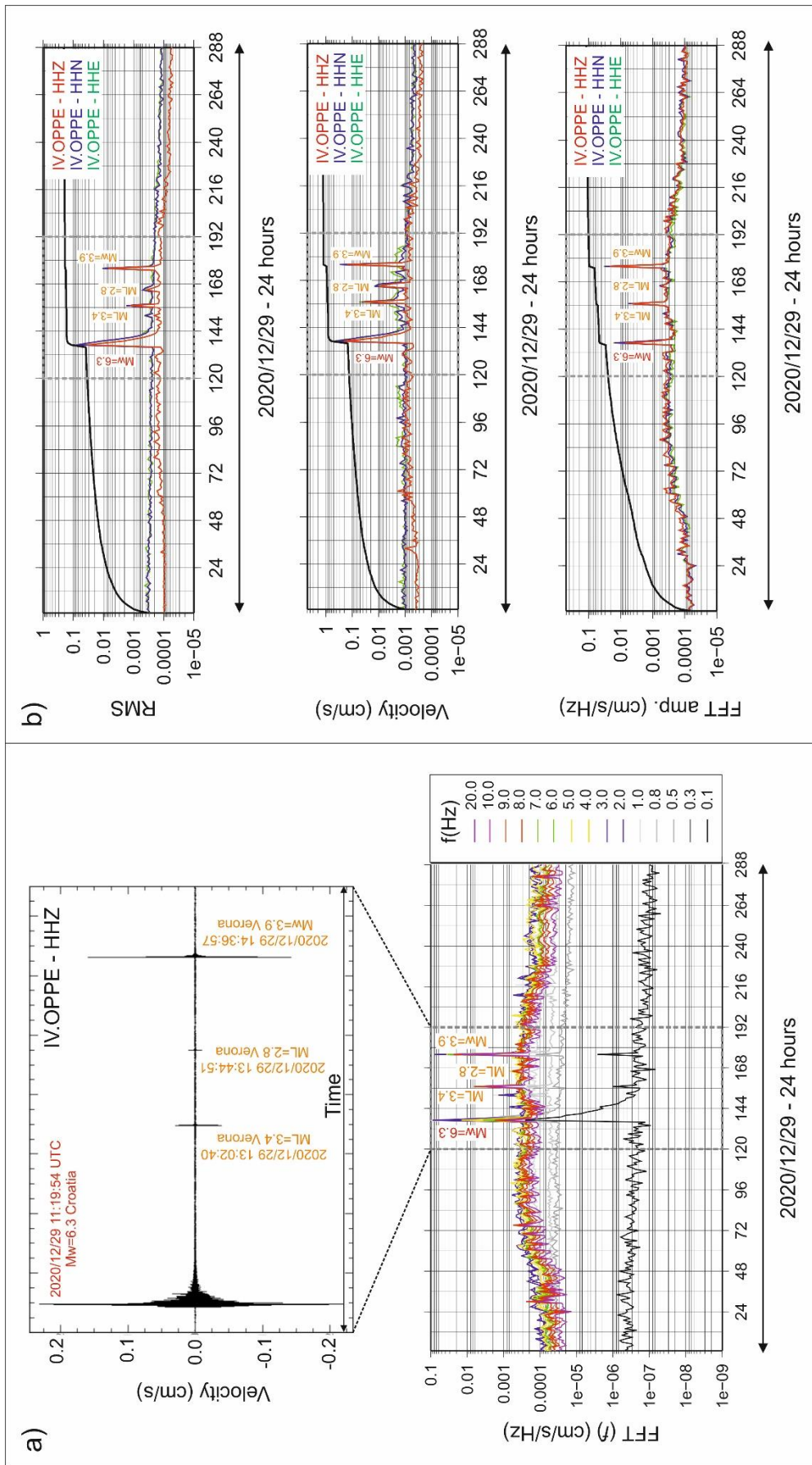
1277

1278

1279

1280

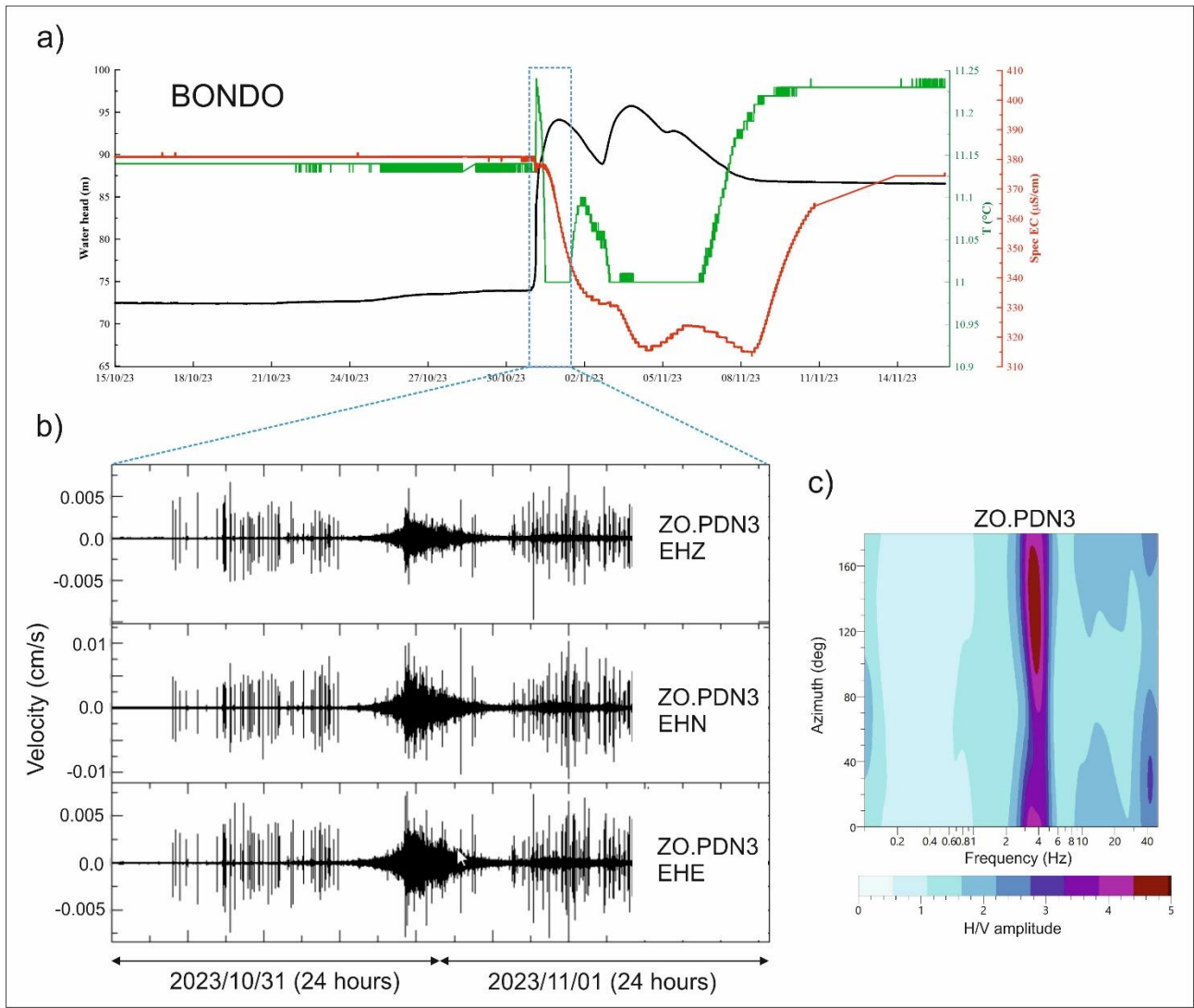
1281



1282

1283

1284 Figure 7



1285

1286

1287 Figure 8

1288

1289

1290

1291

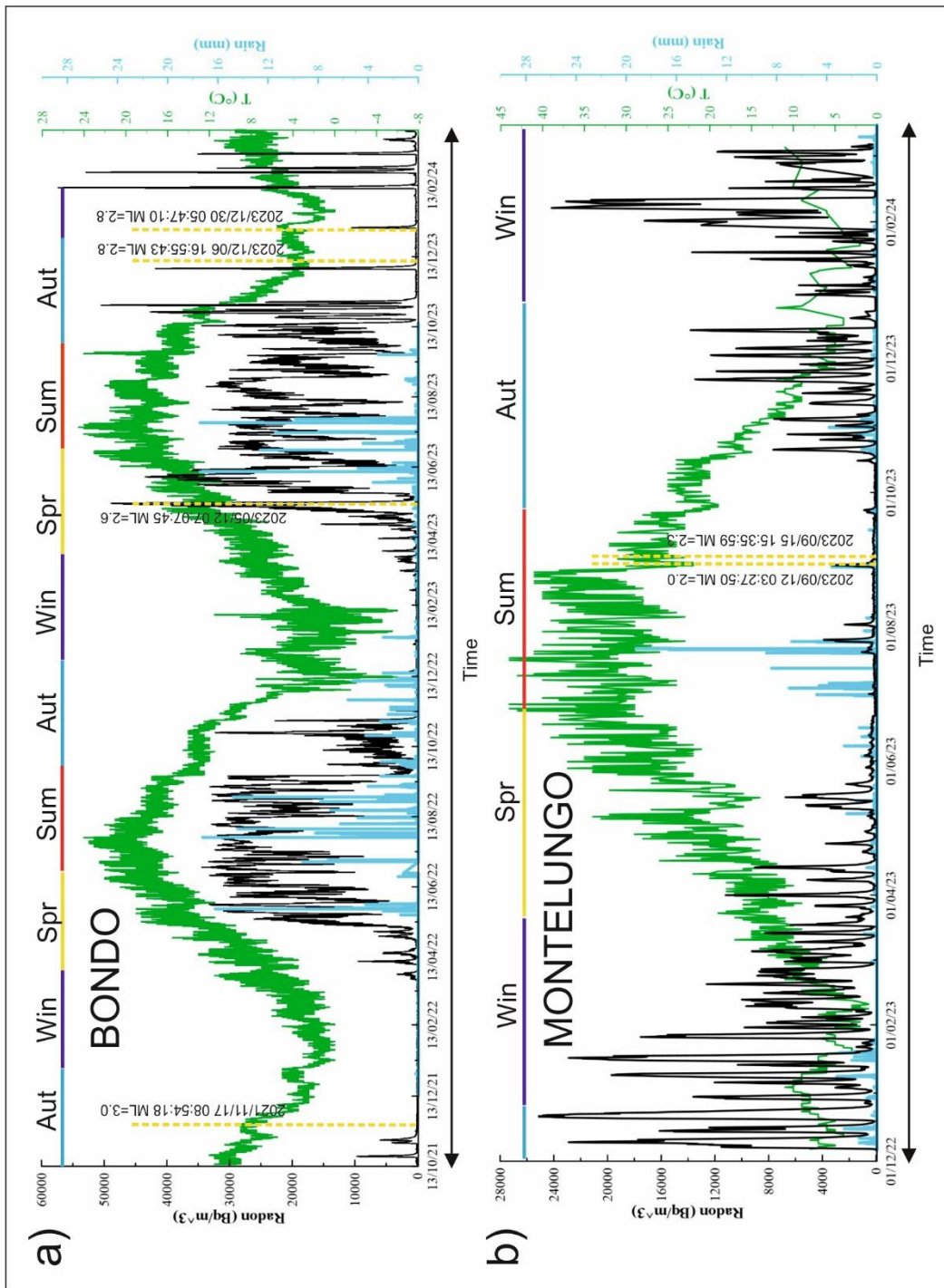
1292

1293

1294

1295

1296



1297

1298

1299 Figure 9

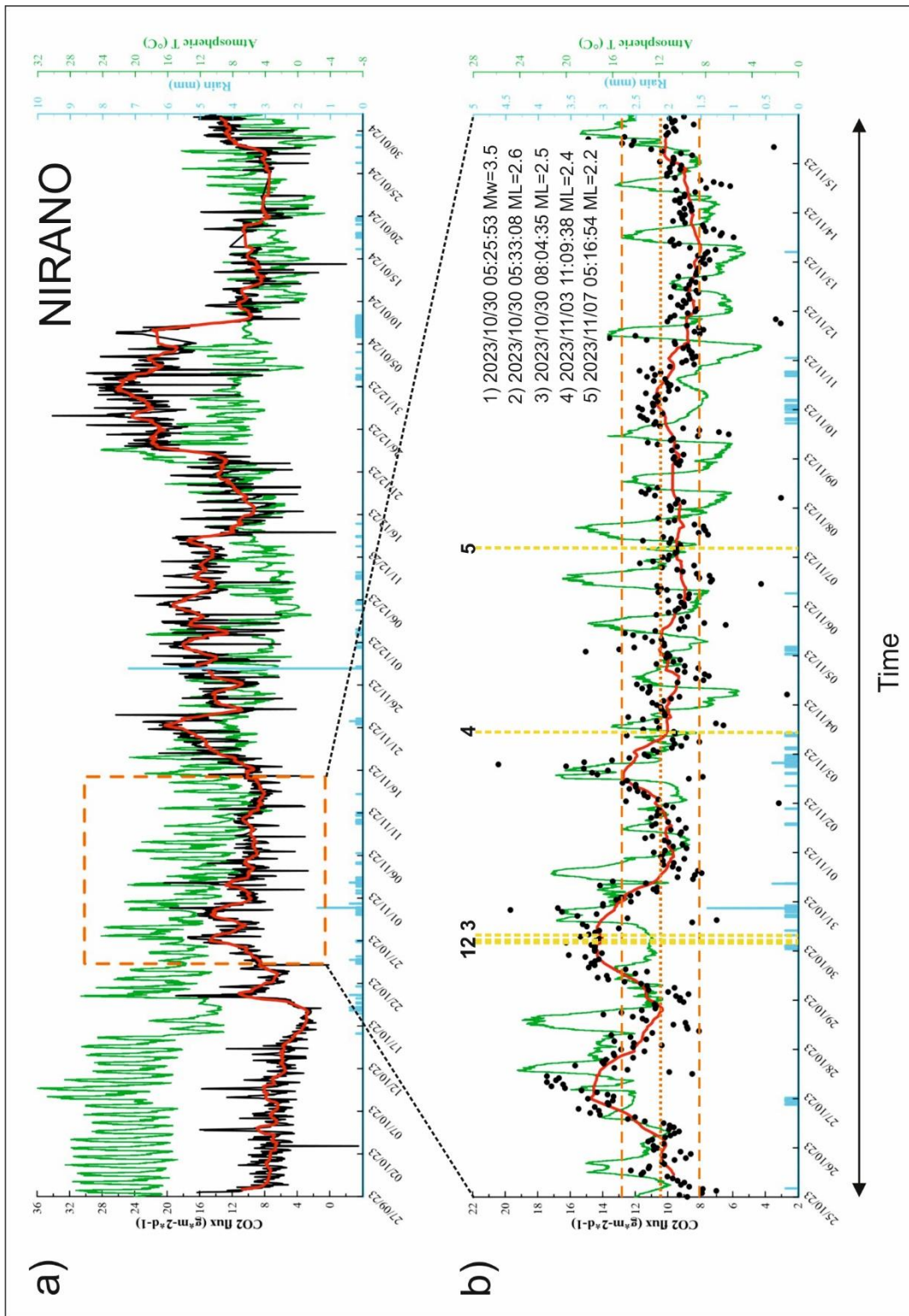
1300

1301

1302

1303

1304



1305

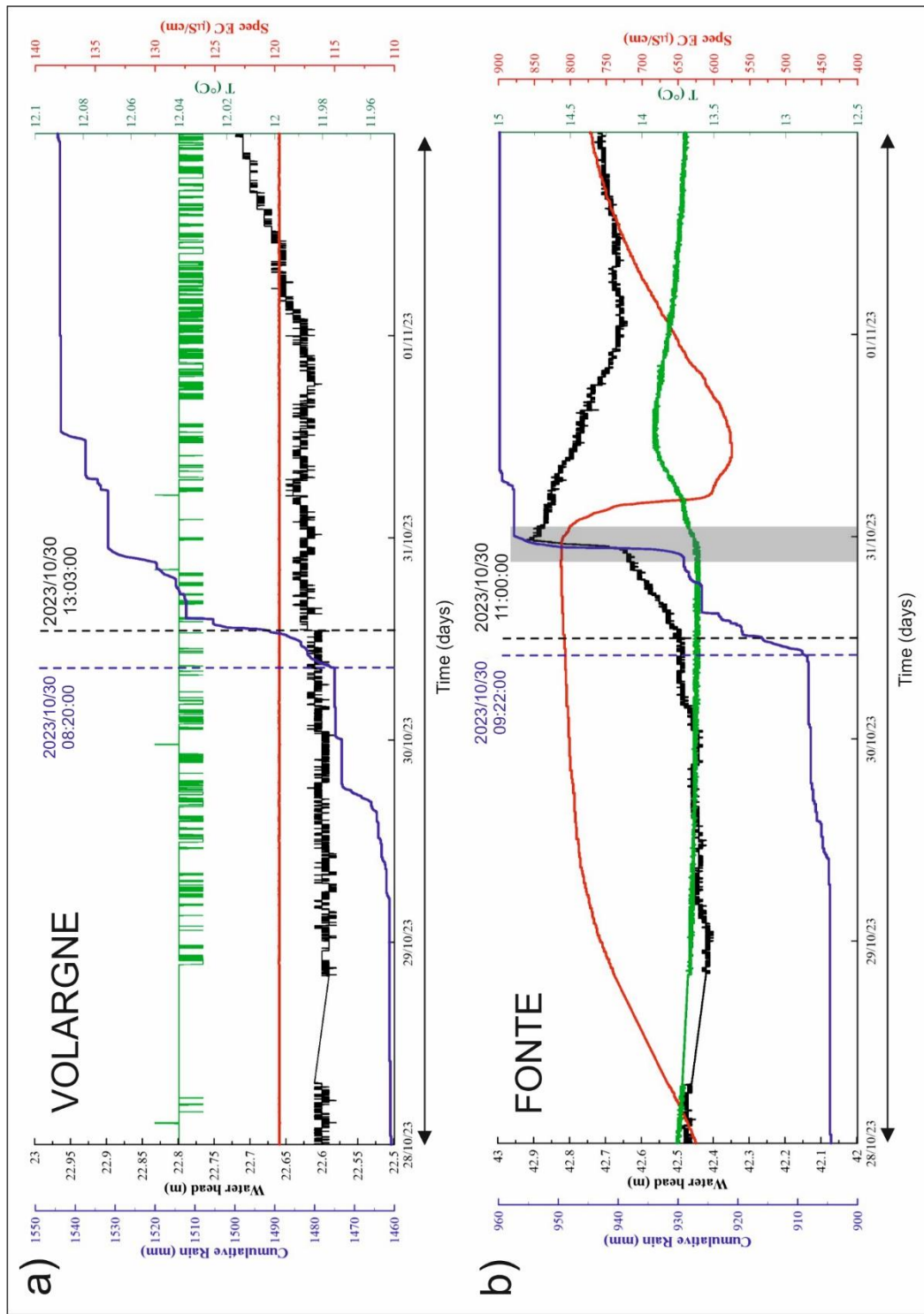
1306

1307 Figure 10

1308

1309

1310



1311

1312

1313 Figure 11

1314

1315

1316

Table 1

CODE	Municipality	AREA	LAT [°]	LOn [°]	idro-geochemical	weather	seismic	Radon	CO2
BALCONI	Pescantina	1	45.4974	10.8763	start 2021-09-23	start 2022-05-26	start 2021-07-13	/	/
BONDO	Tremosine	1	45.8129	10.7377	start 2021-10-13	start 2021-12-13	start 2021-07-22	start 2021-10-14	/
BULGARELLI	Medolla	3	44.8498	11.0627	start 2024-02-28	start 2024-02-28	start 2012-11-28	/	/
CASAGLIA	Ferrara	3	44.9036	11.5406	start 2022-07-29	start 2022-07-29	start 2013-02-08	/	/
CESENA	Malacoda Forli	4	44.2031	12.1855	start 2024-02-20	/	start 2003-03-01	/	/
FELTRE	Feltre	2	46.0107	11.9511	start 2024-02-20	/	/	/	/
FRONTE	Fonte	2	45.7949	11.8697	start 2023-04-18	start 2023-04-17	start 2011-11-17	/	/
GERE	Gardone Riviera	1	45.6422	10.5484	start 2021-10-12 - end 2022-07-30	start 2021-12-02 - end 2023-03-25	start 2021-10-12 - 2023-01-18	/	/
MASER	Maser	2	45.7969	11.9658	start 2023-04-17	start 2023-04-17	start 2011-11-17	/	/
MEDOLLA	Medolla	3	44.8492	11.0734	start 2024-02-20	start 2024-02-28	start 2012-11-28	/	/
MILANO	Milano	3	45.4972	9.1812	start 2024-03-12	start 2024-03-12	start 2012-01-27	/	/
MIRANDOLA	Mirandola	3	44.8812	11.0782	start 2024-02-23	start 2024-02-23	start 2012-11-28	/	/
MONTELUONGO	Desenzano del Garda	1	45.4429	10.5256	start 2021-09-14	start 2021-11-30	start 2021-07-30	start 2022-12-06	/
NIRANO	Fiorano Modenese	4	44.5141	10.8255	start 2023-04-04	start 2023-06-06	start 2023-06-23	/	start 2023-09-27
NIRANO1	Fiorano Modenese	4	44.5002	10.8163	start 2024-02-20	start 2024-02-20	start 2023-06-23	/	/
NORCIA	Norcia	5	42.7838	13.1201	start 2023-12-11	start 2023-12-11	start 2023-12-04	start 2023-12-11	/
OPPEANO	Oppeano	3	45.3082	11.1723	start 2023-06-29	start 2023-06-21	start 2023-02-16	/	/
RECOARO	Recoaro Terme	1	45.6998	11.2217	start 2024-01-30	start 2024-01-30	/	/	/
RECOARO1	Recoaro Terme	1	45.7005	11.2215	start 2024-01-30	start 2024-01-30	/	/	/
RENAZZO	Renazzo	3	44.7624	11.2836	start 2024-02-20	/	start 2003-10-11	/	/
SECCHIA	Concordia Secchia	3	44.9245	11.0183	start 2024-03-14	start 2024-03-20	start 2012-11-28	/	/
TOPPO	Toppo di Travesio	2	46.1985	12.8171	start 2024-02-25	/	/	/	/
TRIPONZO	Triponzo	5	42.8400	12.9480	start 2023-12-12	start 2023-12-12	start 2023-12-04	start 2023-12-12	/
VERONELLO	Bardolino	1	45.5098	10.7645	start 2021-09-14 - end 2022-08-01	start 2021-10-19 - end 2023-04-07	start 2021-07-08 - end 2023-04-07	start 2021-12-17 - end 2022-07-08	/
VOBARNO	Vobarno	1	45.6428	10.5035	start 2023-03-10 - end 2023-06-21	start 2023-03-10 - end 2023-06-21	start 2021-07-08	/	/
VOLARGNE	Dolcè	1	45.5397	10.8235	start 2021-12-16	start 2022-05-20	start 2022-04-12	/	/

CODE	AREA	Geology (100k)	Topography	SITE TYPE	WELL DEPTH (m)	WATER LEVEL (m)	WATER COLUMN (m)	WATER TEMPERATURE (°C)	WATER SPECIFIC EC ^c (µS/cm)	WATER PUMP	SEISMIC NET	SEISMIC CODE	RECORDER	SENSOR
BALCONI	1	fluvio-glacial deposits	plain	well	100	53.3	46.7	14.1	873	1	ZO	PDN2	Lumitek ATLAS	TELLUS-5s
BONDO	1	alluvial deposits	valley	well	180	44	136	11.1	377	0	ZO	PDN3	Reftek-130	LENNARTZ-5s
BULGARELLI	3	alluvial deposits	plain	well	8	1.5	6.5	14.5	2639	1	IV	CAVE	GAIA2	TRILLIUM-120s
CASAGLIA	3	alluvial deposits	plain	well	130	3.5	126.5	17.2	3616	0	IV	FERS	GAIA2	TELLUS-5s
CESENA	4	alluvial deposits	plain	well	8.3	3.1	5.2	16.0	1338	0	IV	BRSN	GAIA2	LENNARTZ-1s
FELTRE	2	limestone	relief	spring	/	/	/	13.4	488	0	/	/	/	/
FONTE	2	sandstone	relief	well	120	7.7	112.3	13.5	840	0	IV	ASOL	Lumitek ATLAS	TELLUS-5s
GERE	1	fluvio-glacial deposits	valley	well	60	31.3	28.7	10.3	406	1	ZO	PDN6	Lumitek ATLAS	TELLUS-5s
MASER	2	sandstone	relief	well	157	71.3	85.7	13.2	511	0	IV	ASOL	Lumitek ATLAS	TELLUS-5s
MEDOLLA	3	alluvial deposits	plain	well	50	3	47	15.3	5190	0	IV	CAVE	GAIA2	TRILLIUM-120s
MILANO	3	alluvial deposits	plain	well	152	18	135	14.0	250	0	IV	MILN	GAIA2	TRILLIUM-40s
MIRANDOLA	3	alluvial deposits	plain	well	300	5.4	294.6	17.2	87864	1	IV	CAVE	GAIA2	TRILLIUM-120s
MONTELUONGO	1	morainic deposits	hill	well	150	52.8	97.2	15.3	885	0	ZO	PDN4	Reftek-130	LENNARTZ-5s
NIRANO	4	mudstone	hill	mudhole	11	0	11	16.2	12024	0	ZO	PDN10	GAIA2	LENNARTZ-5s
NIRANO1	4	mudstone	hill	mudhole	11	0	11	14.8	2873	0	ZO	PDN10	GAIA2	LENNARTZ-5s
NORCIA	5	alluvial deposits	valley	well	64	30	34	12.0	535	1	ZO	PDN11	Reftek-130	LENNARTZ-5s
OPPEANO	3	alluvial deposits	plain	well	60	4.6	55.4	13.9	607	0	ZO	PDN9	SARA-SI06	SARA-SS08-120s
RECOARO	1	sandstone	relief	spring	/	/	/	11.4	2148	0	ZO	PDN13	Lumitek ATLAS	TELLUS-5s
RECOARO1	1	sandstone	relief	spring	/	/	/	11.3	3724	0	ZO	PDN13	Lumitek ATLAS	TELLUS-5s
RENAZZO	3	alluvial deposits	plain	well	6	1.5	4.5	17.4	1193	0	IV	RAVA	GAIA2	LENNARTZ-5s
SECCHIA	3	alluvial deposits	plain	mudhole	1	0	1	17.5	2343	0	IV	CAVE	GAIA2	TRILLIUM-120s
TOPPO	2	alluvial deposits	valley	well	300	114	186	12.7	591	0	/	/	/	/
TRIPONZO	5	limestone	crest	well	53	3.1	49.9	29.7	2487	1	ZO	PDN12	Reftek-130	LENNARTZ-5s
VERONELLO	1	fluvio-glacial deposits	hill	well	198	90	108	14.0	703	0	ZO	PDN1	Lumitek ATLAS	TELLUS-5s
VOBARNO	1	alluvial deposits	valley	well	36	11.2	24.8	13.3	240	0	IV	VOBA	Lumitek ATLAS	TELLUS-5s
VOLARGNE	1	fluvio-glacial deposits	valley	well	99	50	49	12.0	129	0	ZO	PDN8	Reftek-130	LENNARTZ-5s

Table 2